BRNO UNIVERSITY OF TECHNOLOGY
VYSOKÉ UČENÍ TECHNICKÉ V BRNĚ

FACULTY OF MECHANICAL ENGINEERING
FAKULTA STROJNÍHO INŽENÝRSTVÍ

INSTITUTE OF SOLID MECHANICS, MECHATRONICS AND BIOMECHANICS
ÚSTAV MECHANIKY TĚLES, MECHATRONIKY A BIOMECHANIKY

COMPUTATIONAL MODELLING OF MECHANICAL TESTS OF ANIMAL CELL
VÝPOČTOVÉ MODELOVÁNÍ MECHANICKÝCH ZKOUŠEK ŽIVOČIŠNÉ BUŇKY

MASTER'S THESIS
DIPLOMOVÁ PRÁCE

AUTHOR — **Bc. Lucie Orlová**
AUTOR PRÁCE

SUPERVISOR — **prof. Ing. Jiří Burša, Ph.D.**
VEDOUCÍ PRÁCE

BRNO 2021

BRNO UNIVERSITY OF TECHNOLOGY
FACULTY OF MECHANICAL ENGINEERING

Assignment Master's Thesis

Institut:	Institute of Solid Mechanics, Mechatronics and Biomechanics
Student:	**Bc. Lucie Orlová**
Degree programm:	Applied Sciences in Engineering
Branch:	Engineering Mechanics and Biomechanics
Supervisor:	**prof. Ing. Jiří Burša, Ph.D.**
Academic year:	2020/21

As provided for by the Act No. 111/98 Coll. on higher education institutions and the BUT Study and Examination Regulations, the director of the Institute hereby assigns the following topic of Master's Thesis:

Computational modelling of mechanical tests of animal cell

Brief Description:

On the basis of a comprehensive FE model created in the previous research, some simulations of mechanical tests with cells should be carried out. The candidate will get acquainted with structure of a living cell and possibilities of its computational modelling. It should bring her experience in applications of both continuous and discrete finite element models under large deformations.

Master's Thesis goals:

1. To get acquainted with structure of animal cell, especially of its cytoskeleton, with focus on endothelial cells in blood vessels.
2. To get acquainted with finite element modelling of prestressed tensegrity structures under large deformations.
3. To simulate a chosen mechanical test of isolated animal cell using FE model.

Recommended bibliography:

ETHIER, C. R. and SIMMONS C. A.: Introductory Biomechanics. Cambridge University Press, 2007.

BANSOD, Y. Computational simulation of mechanical tests of isolated animal cells. VUT v Brně, disertační práce, 2016.

Deadline for submission Master's Thesis is given by the Schedule of the Academic year 2020/21

In Brno,

L. S.

prof. Ing. Jindřich Petruška, CSc. Director of the Institute	doc. Ing. Jaroslav Katolický, Ph.D. FME dean

Summary
The presented Master's thesis deals with the structural arrangement of living animal cells and their mechanical behavior under loading. The generalized aim is to describe mechanical responses of cells under either physiological or pathological conditions.

A highly interdisciplinary approach interconnecting the computational methods of solid mechanics (finite element method in particular) with medical research is an inseparable part of the problem solution. A crucial step in proposing a computational model for approximation of a living cell behavior under loading conditions is to establish mechanically significant components to be incorporated into the calculation and to identify their material parameters. A presented computational model incorporates continuum entities such as the nucleus, membrane, and cytoplasm interconnected with a discrete mitochondrial network. This results in a novel hybrid model which is validated through comparison with experimental data and serves as a means to estimate the mitochondrial impact on overall cell stiffness.

Abstrakt
Předkládaná diplomová práce se zabývá stavbou živých živočišných buněk a jejich odezvou na mechanické zatěžování. Zobecněným zaměřením práce je popis mechanického chování buňky nejenom ve fyziologickém, ale i v patologickém stavu.

Výchozím předpokladem pro úspěšné řešení zadané úlohy je vysoce interdisciplinární přístup kombinující výpočtové přístupy mechaniky těles (v tomto případě metodu konečných prvků) s lékařským výzkumem. Nejdůležitějším bodem při tvorbě výpočtového modelu, pomocí něhož je možné aproximovat chování živé buňky při zatížení, je zejména identifikace mechanicky významných komponent a jejich materiálových parametrů. V tomto případě jsou jako mechanicky význačné identifikovány spojité součásti jádro, membrána a cytoplazma, které jsou nově propojeny s prvky diskrétními (mitochondriální sítí) v hybridním modelu, jehož platnost je ověřena pomocí experimentálních dat. Tento model slouží jako podklad k vyhodnocení míry vlivu mitochondrií na celkovou tuhost buňky.

Keywords
mitochondria, structural cell model, mechanical response, indentation test, AFM, computational modeling, cancer cell, pathology

Klíčová slova
mitochondrie, strukturní model buňky, mechanická odezva, indentační zkouška, AFM, výpočtové modelování, rakovinová buňka, patologie

ORLOVÁ, L. *Výpočtové modelování mechanických zkoušek živočišné buňky.* Brno: Vysoké učení technické v Brně, Fakulta strojního inženýrství, 2021. 60 s. Vedoucí prof. Ing. Jiří Burša, Ph.D.

Rozšířený abstrakt

Předkládaná diplomová práce pojednává o možnostech výpočtového modelování živočišné buňky z hlediska mechaniky pevných látek. Hlavním cílem je popis charakteristického chování buňky v reakci na vnější zatížení a návrh strukturního modelu pro simulaci odezvy pomocí metody konečných prvků na specifický typ zatížení (charakteristický pro indentační zkoušku).

V úvodních kapitolách je v literatuře vyhledána a následně představena vnitřní struktura živočišné buňky z biologického pohledu s krátkým popisem rozměrově nejvýznamnějších komponent, který obsahuje informace ohledně jejich rozměrů, rozložení a funkce v rámci individuální buňky. Dále práce předkládá krátké shrnutí procesů probíhajících uvnitř jednotlivých buněk a v návaznosti také pojednává o vybraných patologických procesech, jejichž výzkum je jednou z hlavních motivací pro zpracovávání tohoto tématu.

Úvodní kapitoly jsou doplněny o shrnutí metod vhodných pro zobrazování vnitřní struktury buněk a o přehled metod používaných pro testování mechanické odezvy buněk na vnější zatížení. Pozornost je věnována zejména vypracování detailního rozboru indentační zkoušky, která je uskutečňována pomocí vtlačování hrotů různých tvaru do buňky a pomocí citlivých senzorů určuje odezvu na takovéto zatížení. Tato zkouška byla zvolena jako prostředek pro verifikaci předkládaného modelu. Všechny experimentální přístupy jsou však interdisciplinárně zajímavé nejenom z hlediska mechanického, ale i pro své využití v lékařském výzkumu, se kterým toto téma velice úzce souvisí.

Na poznatky o biologické stavbě buněk navazuje kapitola pojednávající o aktuálních možnostech a aplikovaných postupech při výpočtovém modelování mechaniky buňky. Příklady prací zabývajících se mechanikou buňky lze nalézt zejména na Ústavu mechaniky těles, mechatroniky a biomechaniky (ÚMTMB), ale i jinde ve světě.

Jednotlivé přístupy lze rozdělit do několika skupin dle charakteru modelování vnitřního uspořádání. Konkrétně lze rozlišovat mezi modely kontinuálními, které do výpočtového modelování vkládají vysokou míru nepřesnosti tím, že ať už zcela nebo částečně zanedbávají výraznou heterogenitu buňky, a modely hybridními, které do spojitých částí (mezi něž se většinou řadí jádro, membrána a cytoplazma) začleňují diskrétní prvky jako například cytoskelet.

Součástí řešení zadané úlohy je také identifikace mechanicky významných komponent a zvážení míry významnosti jejich vlivu ve vztahu k celkové tuhosti buňky. Jelikož je úloha definovaná v Zadání diplomové práce zejména úlohou o identifikaci materiálových parametrů jednotlivých komponent začleněných do předkládaného modelu a konstitutivních modelů vhodných pro jejich popis, věnuje se část práce vyhledání těchto charakteristik v literatuře a vytvoření jejich stručného přehledu, který je tak výchozím bodem pro modelování metodou konečných prvků. Zde je vzhledem k velkému rozptylu materiálových parametrů poukázáno na výhodné využití kontinuálních modelů pro snadnou a časově nenáročnou manipulaci, a tedy vhodnou volbu a verifikaci materiálových parametrů pro aktuální nastavení úlohy.

Většina hybridních modelů představených v předchozích výzkumných pracích se zaměřuje na mechaniku opěrné soustavy buňky: cytoskeletu, která je zodpovědná za většinu tuhostních charakteristik buňky. Důvodem je, že vlákna tvořící cytoskelet, jsou nejtužším prvkem ze soustavy buněčných komponent a jejich uspořádání je zodpovědné za významné deformační zpevnění, které buňka při experimentálních měřeních vykazuje. Modely cytoskeletu většinou využívají tzv. tensegritních (tedy uzavřených

samonosných) struktur, které jsou v textu nejenom definovány, ale navíc je popsán jejich význam v rámci mechaniky buňky.

Jedinečnost této diplomové práce v oboru a její příspěvek k dalšímu výzkumu spočívá v charakteru diskrétních prvků začleněných do struktury navrženého modelu. Na základě poznatků výzkumu na Masarykově univerzitě je vyslovena domněnka, že kromě významného vlivu jádra, cytoplazmy, buněčné membrány a cytoskeletu na mechanickou odezvu buňky, mohou i mitochondrie přispívat k celkové tuhosti buňky. Konkrétněji byla pozorována reorganizace (v podobě rozpojování a řídnutí) mitochondriální sítě v buňkách ovlivněných rakovinou, při které je paralelně ovlivněna celková tuhost buňky. K ověření domněnky, že mitochondrie mohou ovlivňovat celkovou tuhost buňky nezávisle na dalších změnách ve struktuře buňky, je posléze využito nového hybridního modelu zahrnujícího realistickou mitochondriální síť.

Platnost předkládaného modelu je na závěr ověřena pomocí simulace zatížení, které odpovídá indentační zkoušce sférickým hrotem, a porovnáním výpočtové odezvy s experimentálními daty. Celková tuhost buňky předkládaného modelu je vyhodnocována jako reakční síla působící na indentační hrot v několika indentačních bodech podobným způsobem, jako při experimentálním ověřování.

Výpočty provedené v rámci této diplomové práce naznačují, že mitochondriální síť ovlivňuje mechanickou odezvu buňky poměrně významným způsobem. Z toho vyplývá, že změněná (ať už zvýšená či snížená) tuhost rakovinových buněk může být kromě jiného úzce spjata s reorganizací mitochondriálního systému.

I declare that this thesis has been composed solely by myself and that it has not been submitted, in whole or in part, in any previous application for a degree. Except where stated otherwise by reference or acknowledgment, the work presented is entirely my own.

Bc. Lucie Orlová

I would like to express my special thanks of gratitude to prof. Ing. Jiří Burša Ph.D. for his never-ending patience and much appreciated guidance during the time of preparation of this thesis. I am also extremely grateful for the opportunity of having met MUDr. Jaromír Gumulec, Ph.D. whose different point of view and scientific advice inspired many ideas presented within the chapters.

My thanks also goes to Veera Venkata Satya Jakka, M.Sc., Ing. Jiří Vaverka and Ing. Petr Lošák, Ph.D. who helped to point me in the right direction whenever was necessary. The completion of this project would not be possible without the support from Bc. Tomáš Jadrný. Last but not least, I would like to thank my parents and friends who helped me a lot in finalizing this project within the limited time frame.

Finally, I humbly appreciate the pleasant environment and the human touch that I have encountered through all of my studies on FME BUT so far. I will try to utilize all of the gained experience in my future work and research.

Bc. Lucie Orlová

Contents

1. Introduction

The complexity of the cell which is a basic unit of every living tissue is astonishing. The cell structure is highly heterogeneous: it is composed of several components that influence its mechanical response to loading conditions making the description and subsequent evaluation of isolated cell mechanical behavior a complex research chapter requiring an interdisciplinary approach.

The inner structure enables the cell to undergo long-term as well as temporal loading by constant adaptation so the load is transferred through the cell without damaging the vital parts. The important part about maintaining the internal force balance is that the mechanical stimuli are converted to biochemical signals [3] causing a variety of processes to initiate.

With increasing imaging resolution it is feasible to observe and assess the geometry of a variety of those reinforcing cell components thoroughly and even incorporate them subsequently into a complex computational model to determine the impact of such components and their arrangement on overall cell response. Understanding the cell's inner structure could one day result in explaining pathological processes occurring within cells which would lead to discovering means of preventing undesirable cell changes (usually caused by a disease such as atherosclerosis [6], cancer [21], etc.). The undesirable effects can be triggered either by whole tissue structural changes or, at a smaller scale level, changes in cell architecture (e.g. components rearrangement) [34]. The systematic assessment of the cell stiffness can serve not only as a mean of deteriorated cell identification but also as an indicator of treatment success rate [20].

One of the complications accompanying computational simulation of whole-cell behavior is fairly complicated data acquisition. Even though it is already possible to assess the cell mechanical behavior by a number of experimental methods measuring its overall response when subjected to compression, tension, or shear [3], the assessment of the behavior of individual cell components, especially *in vivo*, still comes as quite a challenge due to the small dimensions and cell components overlap inside the living cell.

1.1. Motivation

The research conducted at the Faculty of Mechanical Engineering of BUT proposed several eukaryotic cell models with diverse topology, geometry and/or material properties which were validated through comparison of a cell test simulation with experimental data measured using the methods known in the field. The previous research provided important information to serve as a base ground for new model formulation. The general objective of this thesis is similar to the topics already elaborated: to investigate the mechanism of cell response to mechanical stimuli. However, a new, updated concept is proposed due to the new ascertained facts that arose during the past few years. Additionally, new cooperation between the Institute of Solid Mechanics, Mechatronics and Biomechanics at BUT and the Department of Pathophysiology at MUNI has been established providing entirely new possibilities for acquiring tailored data on cell morphometry and mechanics.

Problem definition

The generalized aim of this thesis is to formulate a hybrid cell computational model based on the present state of the art and perform its validation using indentation test simulation. Utilize the proposed model to evaluate the mitochondria related difference in the cell stiffness in physiological and pathological state.

1.2. Problem-solving and goal setting

Simulating the cell behavior based on previously unknown/undetermined parameters such as material properties is an inverse problem. The following milestones leading to a successful solution to the problem are established as follows:

1. Perform a literature overview about the inner structure of a eukaryotic cell.
2. Research and summarize experimental methods used for measuring overall cell mechanical response available from the literature.
3. Research and summarize available information on the mechanical properties of cell structural components available from the literature.
4. Get acquainted with finite element (FE) methods used for mimicking cellular mechanics focusing on pre-stressed tensegrity structures under large deformations.
5. Formulate the computational model using the knowledge acquired from literature or other sources. Additionally, based on the information acquired by medical research, incorporate a mitochondrial system into the design with the aim to evaluate its impact on overall cell response to mechanical stimuli.
6. Simulate an indentation test of an isolated cell using the proposed FE model, evaluate and assess the validity of assigned mechanical properties.

As for the choice of software processing tools, they can be divided into separate groups: experimental data processing tools and finite element calculation tools. The former is discussed in detail further in the text. From the variety of ANSYS tools for FEM analysis, the Ansys Mechanical APDL is to be utilized since it allows for greater input parameters control and makes scripting an inseparable part of the calculation setup in comparison with the other packages which is advantageous for adjustment of the model parameters.

2. General background

The cell is a complex living self-sufficient and self-supporting system that allows for every higher living organism to exist. The prokaryotic cells (being separate living organisms such as bacteria) and eukaryotic cells can be distinguished. The eukaryotes are generally characterized by the existence of one or several nuclei at the center of the cell body and they can be found in animals, plants, or fungi (each characterized by unique inner arrangement) [18]. Since the prokaryotes are not subjected to any significant loading, usually dispersed in their environment and not formulating more complex units, only the eukaryotic cells will be discussed. The individual eukaryotic cells formulate clusters (tissues in animal cells) that are capable of complying with diverse functions such as reinforcing, building, or providing nutrition for other systems.

Generally, the free shape of the cell is supposed to be spherical when floating in a liquid environment, but as the tissues comply with different functions, the cell shape differs accordingly. For example, the blood cells with a diameter of several micrometers have a round biconcave shape due to fluid flow (shear) loading [9]. On the other hand, the shape of the arterial wall cell is significantly elongated with a length of a few hundred micrometers which can be explained by predominant tensile loading of the tissue [34]. Nevertheless, the non-specified cells can be classified as round entities of tens of micrometers in diameter which have been observed at cells immersed in a liquid solution. The above-mentioned is illustrated in Figure 2.1

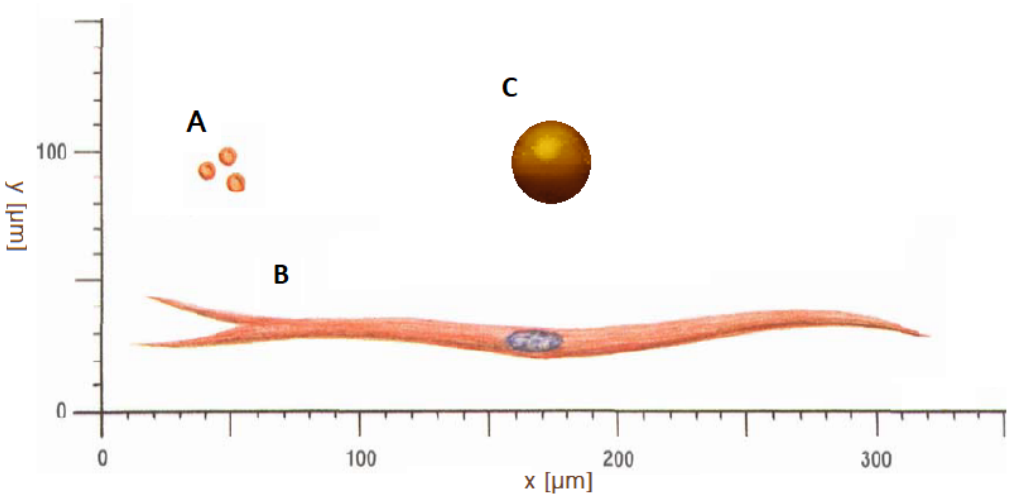

Figure 2.1: Cell shape and dimensions comparison according to their type (function). The red blood cells (A) in comparison with elongated smooth muscle cell (B) and epithelial cell image from AFM contact point map (top view) to illustrate general dimensions of round cells cultivated in a liquid solutions in the adherent state (C). Modified from [9].

2.1. Celular components

The intracellular space covers a variety of usually membrane-type cell organelles each with its own designation and function in a similar manner to cells themselves. The schema 2.2 below illustrates the complexity of cell inner structure in sectional view and is supplemented by the list introducing the most significant organelles of a micro- to nano-level (listed according to their size in descending order).

Membranes

Usually described as a phospholipid double-layer forming a wall enclosing the organelles and thus defining their shape and differentiating them from their surroundings [18]. However it does not separate the components impermeably, the nutrients and other substances are able to pass through the membrane.

The plasma membrane (or cell membrane) is the most significant representative. It is covering the cell body and contributes to cell shape formation. It is approximately 5 to 10 nm thick [3] and serves as an interface for interaction with the surroundings and substance exchange with extracellular space [12]. Since it is not able to withstand significant loading or large deformation, reinforcing layers in the form of the cell endoskeleton (actin cortex) and exoskeleton [25] lay directly beneath and above respectively.

Protoplasm

This term covers all of the entities filling in the space within the cell membrane, i.e. all of the organelles filling the intracellular space including the nucleus. More commonly,

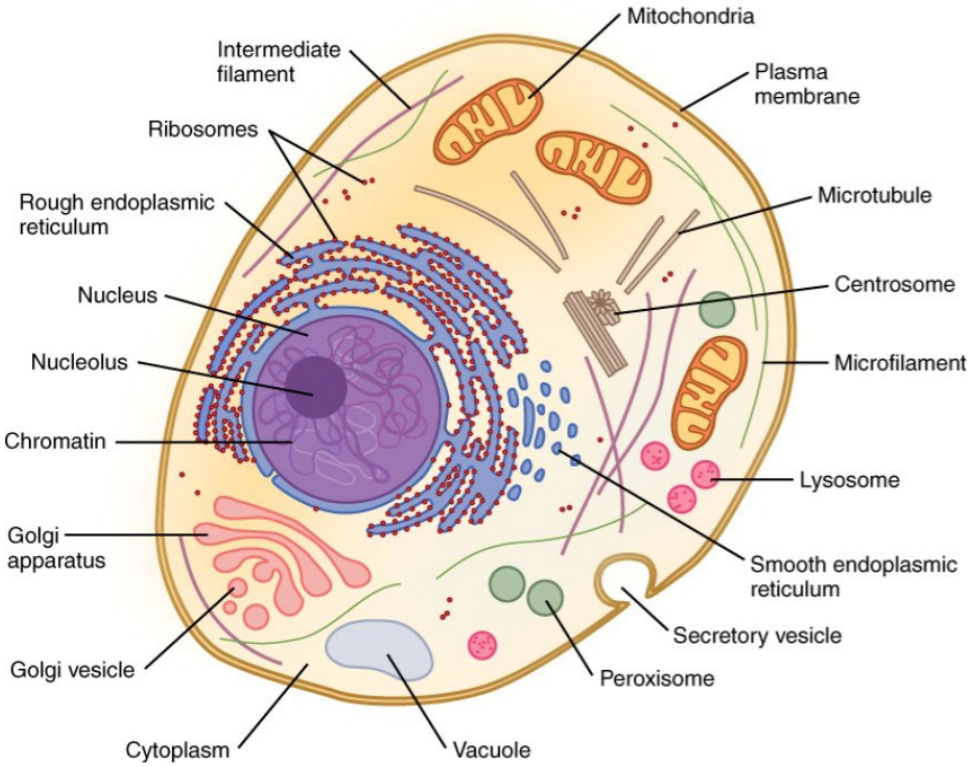

Figure 2.2: Schematics of the cell inner structure in a sectional view, adapted from [12].

the inner space of the cell is referred to as **cytoplasm** which is perceived similarly to protoplasm however nucleus is exempted from the term. The most significant members of cytoplasm are the endoplasmatic reticulum (ER), mitochondria, cytoskeleton, and last but not least cytosol which is a viscous fluid comprising mainly water [45] where other organelles float.

Nucleus

The largest of the cell organelles is formed by its own membrane and nucleoplasm with a diameter up to 20 µm (meaning it occupies a major part of the volume) and is responsible for a significant part of the total mass of the cell [34]. Its function is mainly gene-bearing and chemical response generating and is often associated with the term cell's control center [18].

Endoplasmatic reticulum (ER)

The ER is an organelle composed mainly of interconnected membranes that are responsible for cell metabolism.

Mitochondria

Mitochondria are highly dynamic organelles distributed through all of the cytoplasmatic volume (as illustrated in Figure 2.3) that serves as a "powerhouse" of the cell. Their shape is usually round or oval with a thickness of hundreds of nanometers covered in two membranes as sketched in Figure 2.2. This semi-autonomic organelle is capable of transforming chemical compounds such as glucose [18] into energy resources that are stored in a compound known as ATP (Adenosine Triphosphate) [21]. The energy generated by the mitochondria is used either for cell motion, the molecular exchange with extracellular space, or for chemical reactions (e.g. synthesis of molecules [18]).

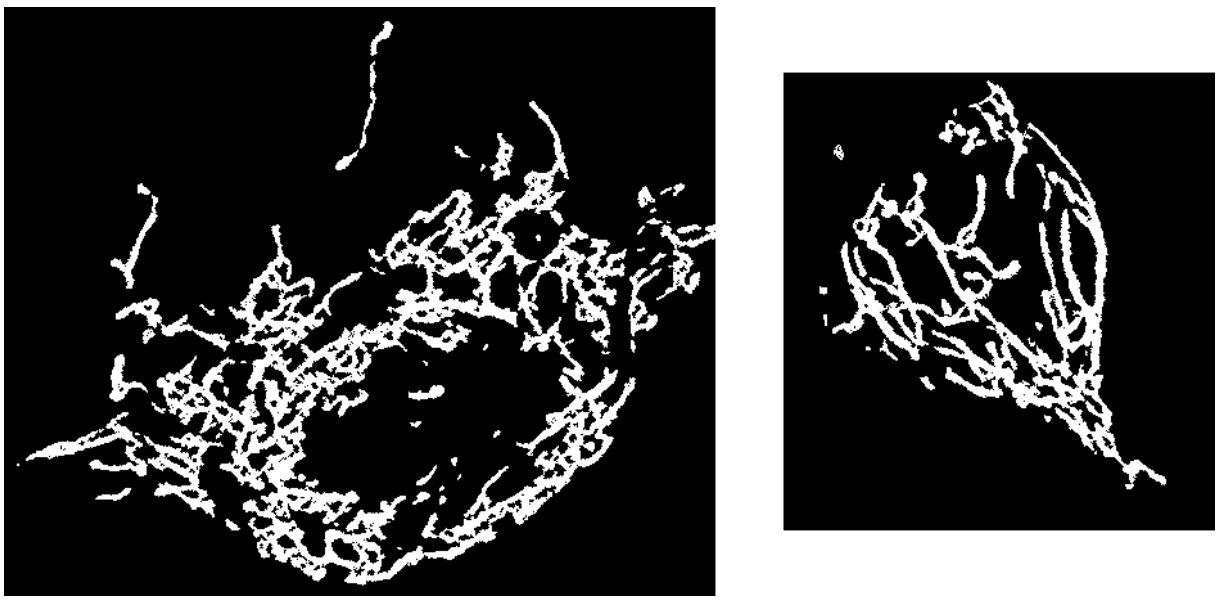

Figure 2.3: A thresholded image of mitochondria distribution in cancer cells (derived from human prostate adenocarcinoma).

Even though mitochondria are reported to occupy only around 10% of the cell volume, they are capable of rapid movement along microtubules and thus traveling through almost the entire cell volume in several minutes [36] in comparison with other organelles such as nucleus which is almost motionlessly fixed to a certain position by a network of microtubules.

Cytoskeleton

Cytoskeleton serves as a reinforcing structure (or a framework [18]) providing the cell with stiffness [39], i.e. active responsive mechanical behavior, and the movement capability by dynamic connection and separation of the fibers. Some of the intracellular components were observed to attach themselves to the cytoskeleton [36], especially to microtubules that serve as a transporting railway. Thus, the cytoskeleton also defines the arrangement of other components.

The cytoskeleton comprises of hundreds of ultrathin protein fibers [18, 41] with the diameter in the order of several nanometers, for comparison approximately 10 times thinner than mitochondria. They can be distinguished into separate groups according to their allocation, state, and mainly their different function: actin filaments, microtubules, and intermediate filaments. In a similar manner to the mitochondrial system, the cytoskeletal filaments are evenly occupying the cytoplasm [3], as illustrated in microscopy images in Figures 2.4 and 2.5. Note, that the colors of the filaments are not consistent through the sources due to different staining agent choices.

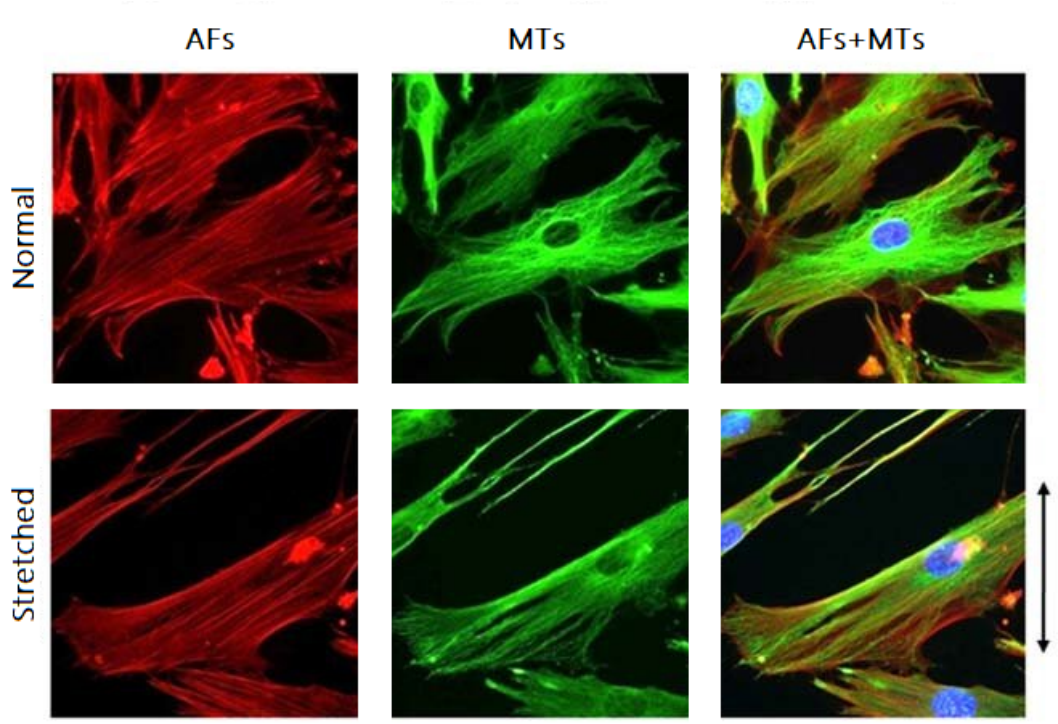

Figure 2.4: Fluorescence microscopy images of cytoskeleton in unloaded state and their adaptation to cycling loading (2 hours of cyclic loading in the marked direction). F-actin (left), microtubules (centre), joined fluorescent image of actin filaments, microtubules and nucleus (right), adapted from [37].

Actin filaments composed of polarized F-actin and G-actin fibers [18] with a thickness of around 5 to 8 nm, usually appear straight (or rather stretched) in the cell body. The static stability of the cell is then generated by pre-stress present in these fibers and the movement capability is dependent on the actin-microtubular network [41].

F-actin fibers are also concentrated around the cell periphery forming a 0.1–1 µm thick layer, i.e. cortical actin or actin cortex [11] and thus supporting the cell membrane [3]. Furthermore, to mechanically interact with the extracellular matrix, the actin forms a complex protein bond with a group of integrins that pass through the plasma membrane [18]. Such bonds are called focal adhesions.

Microtubules are hollow tubes with outer diameter of 25 nm comprising of α-tubulin and β-tubulin [18]. Due to their interaction with actin filaments, they are usually present in a curved state (refer to Figure 2.5) that are growing from and remain attached to an organelle in the proximity of the nucleus called centrosome [34]. Microtubules are, similarly to actin filaments, polarized: the positive end is capable of fast growth while the negative end is attached to the centrosome [41].

Intermediate filaments provide a supporting network for cell stability and ensure nucleus position within the cytoplasm. In a simplified way, intermediate filaments (or IFs) can be visualized as unloaded or wavy fibers that work as safety agents ensuring the cell stability in a loaded state (i.e. they activate under a specific deformation).

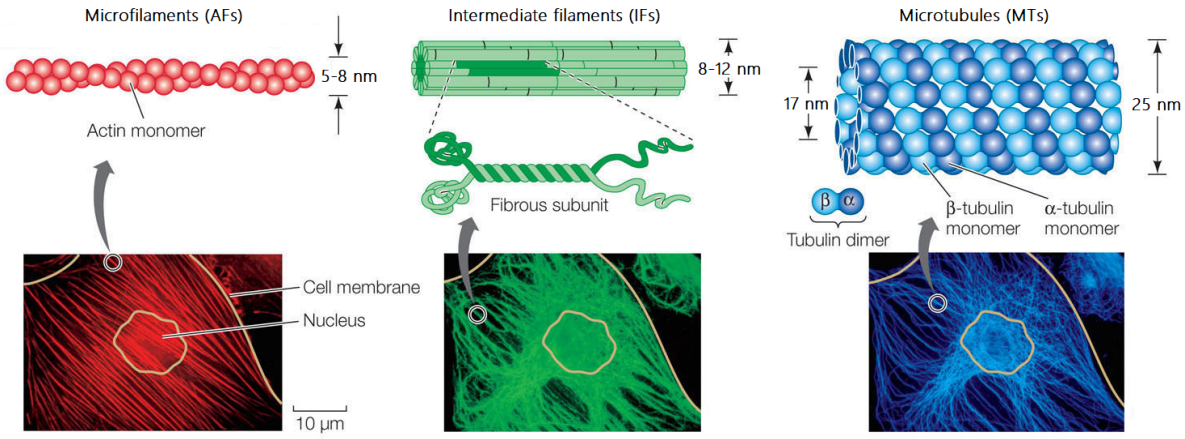

Figure 2.5: The three cytoskeletal filament types, their composition and distribution in cell, adapted from a figure created by J. V. Small [41].

2.2. Mechanotransduction

Mechanotransduction is a process of transforming mechanical stimulus detected at mechanoreceptors (sensory receptors reacting to external stimuli) to the corresponding biochemical response generated by target activation and by its means controlling the cell behavior [18]. It can be perceived as a complex system composed of intracellular components' interaction and chemical reactions occurring within the organelles or on the intracellular matrix compounds such as proteins.

An altered cell environment (including changes in loading conditions as well as chemical disequilibrium) can initiate cell remodeling and therefore probably lays in the center of the pathological processes [34].

2.3. Cell pathophysiology

An important incentive for examining the cell mechanical response lays in explaining the pathological processes occurring in individual cells leading to a global tissue loss or changes in their attributes. Atherosclerosis and cancer can be established as the two main pathologies widely described and investigated.

2.3.1. Cancer

During cancer progression the cell is being reprogrammed, for example, by a piece of genetic information to initiate changes concerning not only its size but also a rapid uncontrolled division [17] (also known as primary tumor formation). Additionally, the cells are able to relocate from a primary to a secondary site. Cancer cells are therefore subjected to various types of loading and energetically demanding processes during cancer progression [21] which result in comprehensive changes in the affected cell's structure.

Apart from a devastating overall impact of cancer on the tissues, it is viable to study the impact of tumor progression on a basis of cellular level or even at a nanolevel of cellular components. It was observed that cancer impacts cytoskeletal architecture [21] as well as its connections to other components, for example, the nucleus as reported in Denais [13]. Other intracellular compartments also reorganize to comply with the altered cellular environment and function.

The changes described above and other possible (not yet described) impacts of cancer processes generally result in varying mechanical properties of cancer cells. It was observed and the primary tumors are softer than the tissue in its physiological state and stiffer in their secondary stages [38].

2.3.2. Atherosclerosis

Atherosclerosis is a disease influencing blood flow in arteries. The substances such as fat or calcium [45] attach to the arterial wall (frequently e.g. in the proximity of arterial bifurcation) and thus block the blood flow. An alteration of loading conditions is augmented by the pulse loading in the blood system and the tissue cells remodel themselves to adapt to such conditions. As a result, the tissue becomes fragile, and affected arteries are susceptible to rupture.

3. Cell-related data acquisition

There are many challenges concerning the study of cell mechanical behavior. The most obvious and significant problem is the scale of dimensions of the object which require high-precision measuring devices as well as high-resolution imaging tools capable of distinguishing not only a cell body as a whole but also the inner structures within it.

The cell commonly undergoes various loading conditions, for example, tension or compression in muscle cells (cells capable of changing the shape by their contraction or relaxation), or shear when subjected to the bloodstream.

Overall, the complexity of cell interaction with various external forces due to its inner structures and processes taking place within the cell body (such as mechanotransduction which is still not completely described) make the interdisciplinary approach utilizing as much of the previous findings as possible the only viable method for expanding the knowledge in the field. Experimental data extraction from a living cell performed in medical laboratories combined with subsequent computational modeling can be used as an example of such collaboration.

The methods designed and utilized for individual cell mechanics testing and possibilities for imaging its inner structure are summarized in the following sections.

3.1. Measuring the cell mechanics

Two types of experimental methods regarding cell examination can be distinguished: cell population testing and single-cell examination [34]. With regard to the Assignment, the cell population tests are not covered in the following summary and only the individual cell tests will be discussed further.

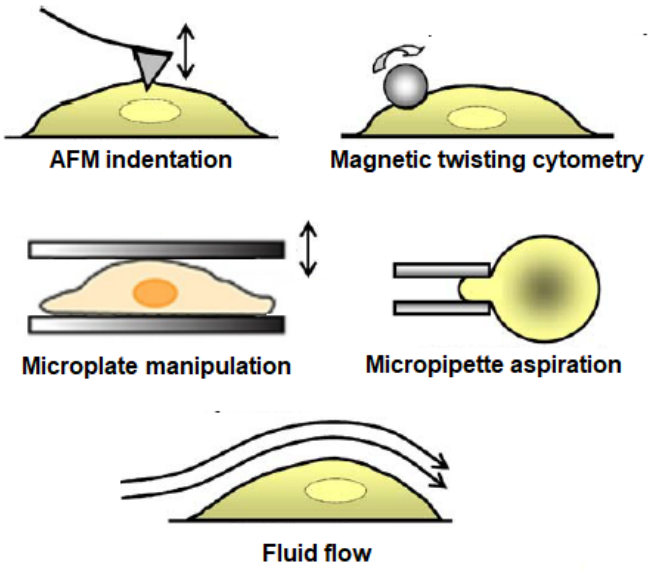

Figure 3.1: Illustrations of various cell testing methods, top row: local methods utilizing probes for the response evaluation, mid and bottom: methods for assessing cell at a macro-level, adapted from [3, 33].

The individual cell testing can be performed by several methods each designed for various types of mechanical loading, either on a global level (e.g. fluid flow, twisting and stretching) or local level, imposing local loading conditions such as point loading [3] aiming at observing the global response to such local deformation [34]. Selected cell testing methods are illustrated in Figure 3.1. Using the methods approaching cell mechanical behavior, a force in the range of several piconewtons to micronewtons [3] or deformation in order of nano- to micrometers (before reaching the value resulting in disrupting the cell body) is applied to the cell body. Such methods are therefore referred to as active methods. The cell can be subjected to dynamic loading as well as static forces mimicking the loading conditions of the cell in a living organism [34], either common in physiology state or possibly occurring during tissue changes.

Nevertheless, all of those approaches focus only on a given part of cell mechanical behavior (resulting from the test load character) which makes finding the universal material model or more specifically, establishing the link between the cell's inner structure and its overall mechanical response, fairly difficult.

Commonly, the desired results to be obtained for a generalized description of the mechanical response are elastic modulus or stiffness of the tested cell (or cell culture). Those are derived indirectly from the force-deformation dependency [28]. Apart from significant variability of the measured reaction force values in different cell cultures, the large deviation of the characteristics measured using different methods aggravates the conclusion-making [3]. A detailed overview of whole-cell mechanical parameters measured derived using different experimental methods can be found in [34].

The Atomic Force Microscopy will be described in more detail in Section 3.1.1 for obvious reasons: it was previously selected as a means for confirming the validity of the proposed computational model. This choice can be further justified by experimental data availability.

3.1.1. Atomic Force Microscopy

The Atomic Force Microscopy (called also AFM, indentation test, nanoindentation test, or else, depending on the publication) is a local method based on the atomic forces between the probe and the examined body that are developed as one body moves closer to the other. It is characterized by extraordinary resolution in comparison with other methods [25]. It utilizes tips, or rather indentors, of various shapes attached to a highly flexible cantilever (the amount of flexibility directly influences the resolution) to probe the surface of the examined body in a vertical direction [3]. The force that acts as a response to the indentation is determined from the cantilever deflection measured by a laser beam (as illustrated in Figure 3.2). The raw (unprocessed) output is in the form of position vs. cantilever deflection curve (see Figure 3.3).

The method was initially designed for observing the general surface or whole-body specifications of solids [25] and apart from utilization for assessing elasticity and viscosity, it is being used also for a surface topography [28], etc. Thanks to the design of the measuring device transcending from general application to utilizing the method in the micro- and nano- environment of the cell does not require much of an adjustment. Its most significant advantage can be found in the possibility to explore the behavior of cell's inner structures (and thus the cell stiffness heterogeneity [20]) by observing as the applied load transfers through the cell body.

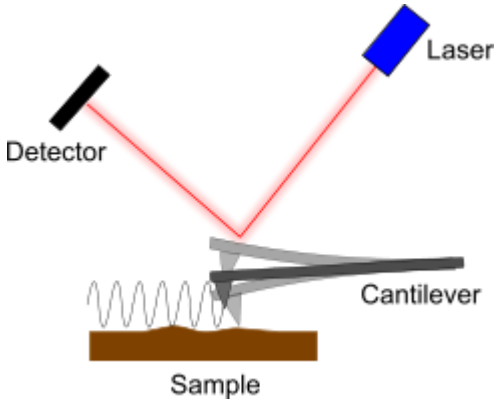

Figure 3.2: Schematics of topography measurement using AFM method, published at Semilab, Germany.

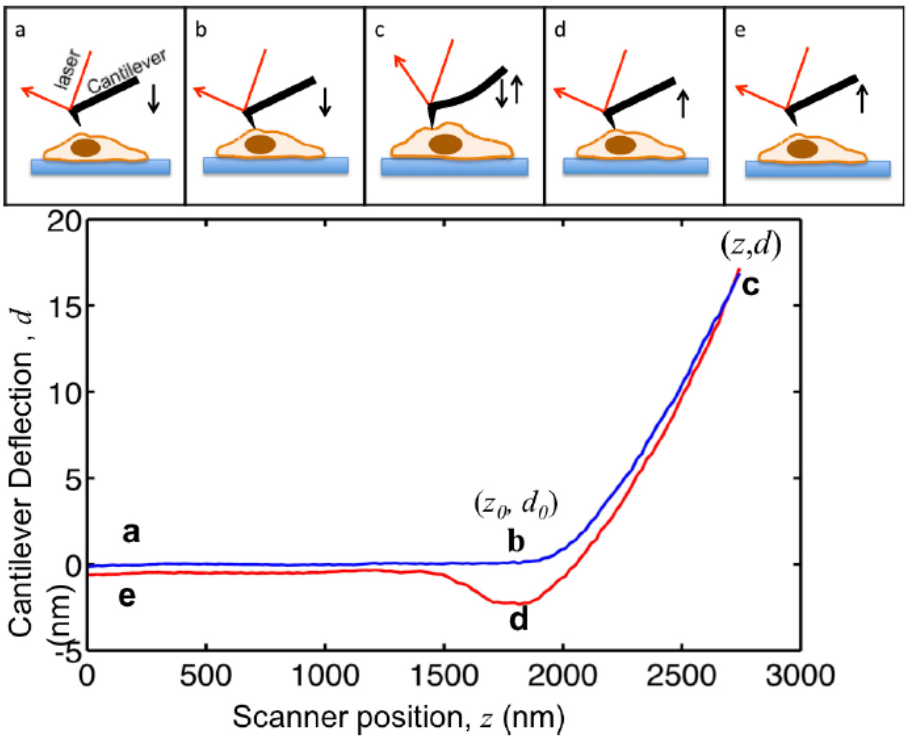

Figure 3.3: The cantilever deflection at an approach phase (blue line) and at withdrawal (red line). Note that the adhesion forces deflect the withdrawing cantilever significantly before its separation from the sample (d), adapted from [20].

Advantageously, the silicon indenters are utilized for the cell indentation since they do not cause excessive mechanotransduction [21] and thus allow for common multi-point data acquisition for a single cell while its response remains consistent meaning the cell does not initiate remodeling processes on a large scale during the test run. The only effect of the indentation is that the components and their cross-links stretch (at most up to the point of breaking) having small to none impact on another indentation site.

Not all of the cell testing methods enable incorporating high-resolution imaging during the test run. This is another advantage of the AFM (implied already in the denomination of the method *Atomic Force Microscopy*), it can be combined with fluorescence and/or electron microscopy (as illustrated in Figure 3.4) to link the inner structure of the currently

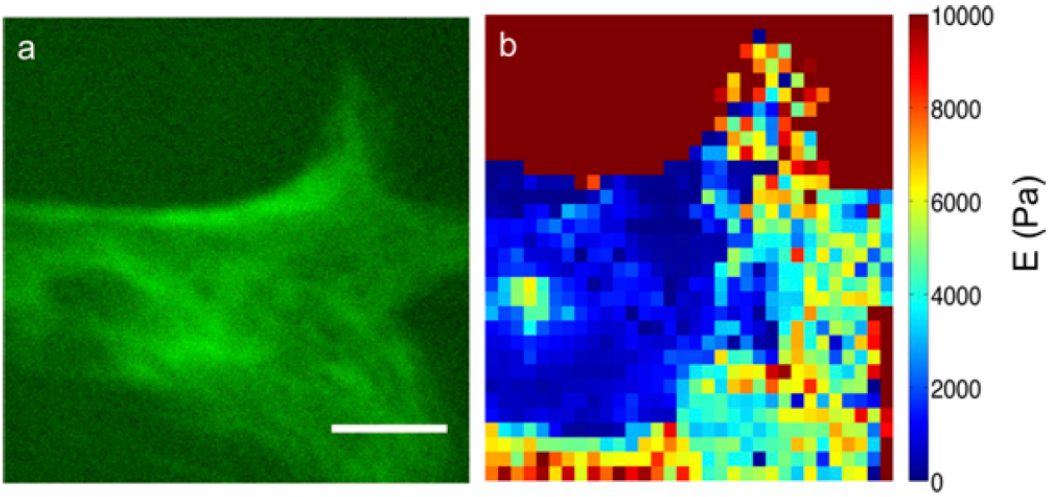

Figure 3.4: Cross-linking the cell inner structure with its point-wise modulus, (a) a microscopy image of a fibroblast injected with a protein highlighting intermediate filaments, (b) a stiffness map extracted by AFM indentation from a fibroblast [20].

examined cell with the possible local stiffness changes [28]. This makes it the most viable high-resolution, high-accuracy method to the day.

Apart from the numerous advantages, it is necessary to mention and specify the limitations of the method. Utilizing the inappropriately set value of loading force can result in damaging the cell as a whole object (by ripping it apart or otherwise damaging its integrity) and thus prematurely terminating the test run. Moreover, if the indentation at a single point is set too large, the evaluated cell stiffness can be affected by remodelation processes initiated within the cell even if the pliable indentors are used [20]. The measurement also provides only with data at a single point at a time [3]. The method is therefore quite time-consuming as the data for one indentation point takes several tens of minutes to extract [21]. This implies that careful design and thorough premeditation of the experiment are essential for obtaining viable results.

The evaluation of the data acquired using the indentation method is based on a simple Hertz theory and its modifications e.g. for adhesive bodies (commonly used for conical indenters) [3] or Sneddon theory for spherical indenters [24], which is being also referred to as the combined Hertz-Sneddon theory. Concisely, the approximations commonly utilized in AFM data evaluation are based solely on fitting a polynomial based on a theoretical formula.

The main disadvantage is that the methods generally do not take into account the cell heterogeneity nor anisotropy and therefore do not allow assessing individual cell components by default. A possible solution to eliminate this deficiency to assess the membrane-underlying structures is illustrated in Figure 3.5. Additionally, most formulas assume the sample thickness being multiple times greater than the indentation depth which is, however, of the same magnitude in cell testing [16]. The assumption is based on the impact of the underlying substrate on the measurement that cannot be neglected, for example, the article by T. Gawain [20] reports noticeable substrate effect from indentation 10% of sample height.

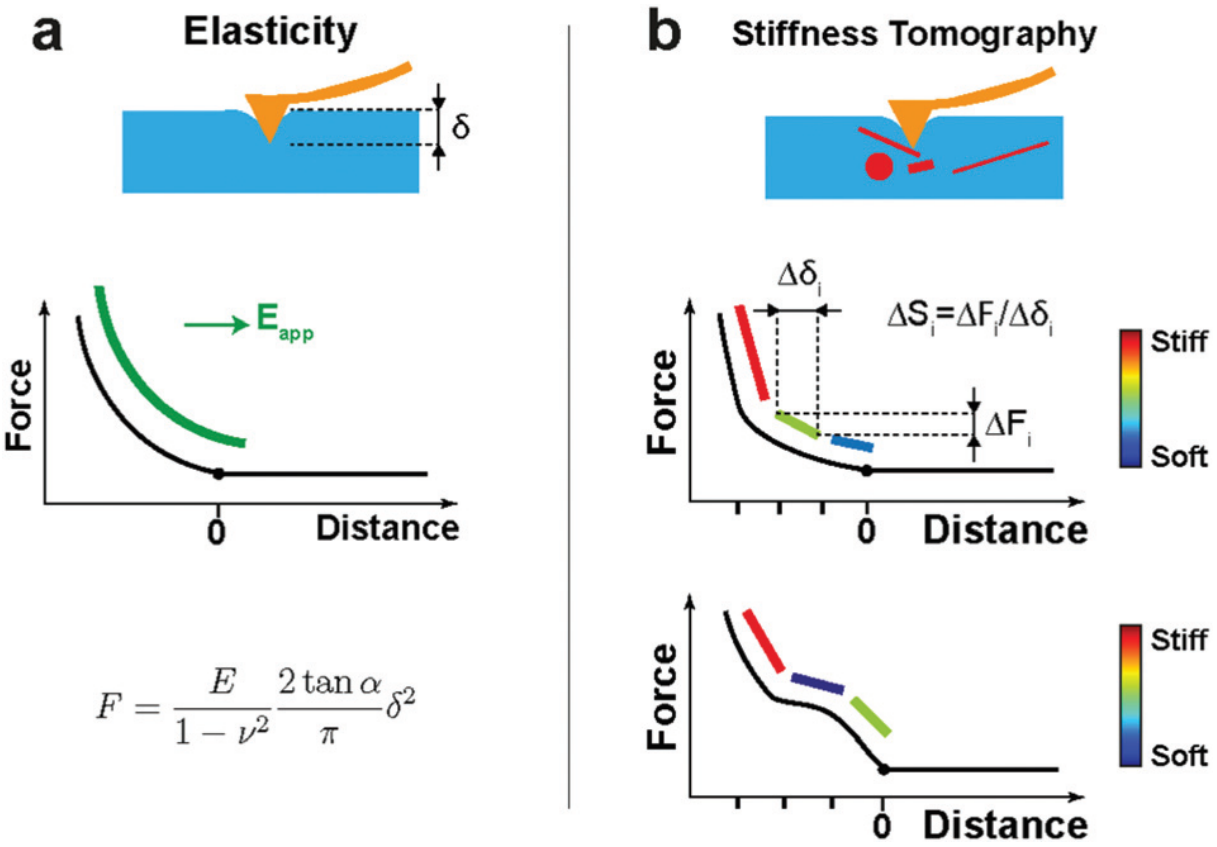

Figure 3.5: The application of the AFM in cell components elasticity measurement. Left: determining the overall cell response by fitting the data by Sneddon's model (where α is a half-angle of the indentor tip, other values as usual), right: the individual cell components affecting the experimental curve at separate regions that can usually be observed as an experimental curve slope change where the approximation by one of the methods is no longer universally valid [28].

3.1.2. Tensile or compression testing

The tensile or compression testing of the cell is usually performed by a pair of micro-pipettes (only for tension) or micro-plates (for tension and compression), which the cell is attached to by adhesion forces [3] or adhesives [25]. One of the probes is fixed and the second one is movable, i.e. actively loads the cell through its movement. The response is measured by a force sensor located on the probes. Thus, the cell is subjected to approximately uniaxial loading.

The micro-plate manipulation is a more universal method of the two that serves as a means to load the cell commonly with compression but it can be also adjusted to shear loading by moving the microplates in transversal direction [25]. The advantage of the micro-plate manipulation is its versability: apart from static loading conditions either by gravitational or other mechanical force, it is possible to apply cycling loading. However, its usage is limited by the cell's capability of creating adhesion forces with the plate.

3.1.3. Magnetic twisting cytometry

This method utilizes the magnetic field generated in a microsphere (bead) embedded in a surface of the cell [20]. The bead is exposed to a torsional magnetic field which causes it to rotate and therefore deform the cell [4].

3.1.4. Micropipette aspiration

This method utilizes micropipettes similarly to the tension test, however, the micropipette is a hollow tube and the cell is being sucked into its opening, that is, by applying negative pressure to the cell membrane studying the elasticity and viscosity of the cell [20, 34].

3.1.5. Fluid flow

During the test run, the cell body is loaded by flowing liquid exposing the cell body to shear [34]. A common purpose of testing cell response under fluid flow is to characterize biochemical processes occurring within the cell.

3.2. Cell imaging

It is desirable to link the cell behavior with the inner arrangement to possibly justify the irregularities in the mechanical behavior. For cell inner structure imaging to be possible, methods incorporating microscopes with large zoom and resolution are required. Since the list of methods that meet resolution requirements is lengthy and new ones are developing rapidly, and furthermore characterizing them is not a constituent part of the researched topic, only those considered relevant, commonly used, or in any way utilized in data acquisition are briefly described. Some of the methods can be even combined to obtain better results (such as confocal microscopy with fluorescent-protein staining).

The methods all have one thing in common, that is, their full potential can be appreciated especially when aided by computer processing tools (machine learning algorithms) eliminating human-induced error while evaluating the acquired datasets [21]. However, the focus of the imaging is the deciding factor when choosing which technique to select. The two main branches are optical microscopy and electron microscopy that vary substantially, especially by resolution. The optical microscopy is described in detail below in Section 3.2.1. The electron microscopes utilize a beam of electrons instead of light. They can zoom in up to a nanometer, whereas optical microscopes differentiate in tenths of micrometers [29, 48].

3.2.1. Optical (or light) microscopy

This technique is based on the magnification of the object using the light reflected or passing through. As indicated above in Section 3.2, the resolution is sufficient to image only large compartments such as the nucleus or larger mitochondria.

Fluorescence imaging

Using the fluorescence imaging method, it is possible to perform the differentiation between structures is possible by the light of specified wavelength exciting response in

proteins which emit light of a different wavelength than the source light [48]. In the particular application of cell imaging, the highlight is performed artificially by an infusion of fluorescent protein into the cell body to highlight certain structures within the cell (with identical chemical composition), for example microtubules, nucleus, or actin fibers in a controlled manner [23]. It is even possible to combine various fluorescent proteins within one imaging (to highlight multiple entities at once). The question of whether and at what rate it influences cell mechanical behavior arises [20, 23].

Confocal microscopy

Confocal microscopy utilizes the concentrated light beam which is advantageous due to higher resolution when compared with conventional fluorescence microscopes. The indisputable advantage of confocal microscopy is the ability to create not only slices as in fluorescence imaging but also three-dimensional representations [29]. The images can be acquired continuously, i.e. over a larger time scope, thus creating time-lapses and enabling observation of changes in cell structure over time. To be noted, the image per second frequency is too long to capture the dynamic nature of molecular processes and it is not possible to improve it significantly since it depends on light speed [48].

Phase contrast imaging

One of the most recent methods bearing a great potential for further use when researching the topic of cell mechanics is Quantitative Phase Imaging (or QPI) [21]. It is based on measuring light phase shift after passing through the object.

4. Present state of art

During the years of research at the Institute of Solid Mechanics of BUT focusing on cell mechanics, the field of finite element modeling advanced rapidly and its possibilities became much broader. Various non-structural as well as structural models have been created and validated there, for further details on proposed models refer to the publications themselves [2, 3, 5, 25, 27, 31, 34, 45]. The following chapters are elaborated with the main reference to those originating at the Institute, even though this does not mean the advances did not occur elsewhere as well.

The cell computational modeling aims to simulate mechanical response and discover all of the factors having an influence over it. Once again, it is to be noted, that most of the computational models built on the ground of experimental data are designed for a particular data set measured by one particular experimental method. The adjustment for different cell measurements is usually possible by changing the parameters of the model, however, the validity of the model for a different experimental method is not always proved.

Some of the important attributes of the cell as a complex unit are listed below. The computational models attempt at capturing them all to a certain extent or including some of them while neglecting others (commented in the following sections).

- **Strain stiffening**: the cell stiffness depends on the stress intensity [3].
- **Cell structural heterogeneity**: the cell comprises of sub-structures with different material properties (continuum approaches neglect the cell heterogeneity whereas microstructural approaches include it).
- **Complexity of material behavior** such as viscoelasticity, adhesiveness, and significant non-linearity [25].

The base steps of computational model definition can be established as significant components identification, material properties assignment, the definition of a computational model and the simulation itself (by subjecting the model to external loading conditions), and finally a comparison of the simulated results with experimental measurements and possible adjustment of the model eventually leading to the validation of the proposed model [25]. The following sections are arranged in the order stated above.

4.1. Mechanically significant components

The identification of the components significantly contributing to the overall mechanical response is a crucial step while establishing the cell computational models. As already implied in the previous chapters, cell nucleus, membrane, cytoplasm, and cytoskeleton with tensegrity structure character (refer to Section 4.3.1 for further details) are usually assumed to play a vital role in cell mechanical response either due to their important dimensions and reinforcing or shape-maintaining function.

4.1.1. Assumptions and hypothesis

Respecting all of the research made in modeling cell response, the mitochondrial network is being added to the list of entities that influence the cell behavior on the background that cell stiffness and mitochondrial system changes were observed in cancer-affected cells. The changes in mitochondrial network in fibroblasts were observed during ongoing research at the Department of Pathophysiology, Faculty of Medicine MUNI. Cancer cells are also showing to have different stiffness than healthy cells which has been always associated with rearrangement of cytoskeleton [21].

Nevertheless, mitochondrial images show, that the mitochondrial system undergoes noticeable geometry rearrangement. This simple observation resulted in a series of experiments on living cells trying to prove whether or not can this change lead to cell softening or hardening [21, 38]. To this day, the mitochondrial changes and cell stiffening have not been correlated yet by a manner of simulation, calculation, or any other method. A possible approach is proposed herein.

The assumption, that mitochondria influence the whole-cell behavior while no other change in cell structure is performed was therefore introduced and it is attempted in the following pages to express inclination towards confirmation or disproval.

4.1.2. Mechanical properties of given components

Even though nowadays it is possible to cultivate and separate different cultures of cells in a physiological and pathological state, measuring mechanical properties (particularly those of individual cell's morphological components) still comes as quite the challenge and the results are often biased due to manual evaluation, i.e. human error [21].

Experimentally determined elastic parameters introduced in the sources differ significantly with the measuring method (see Section 3.1), the method's accuracy, as well as the type of the cell culture assessed and the size of the statistic sample. It is almost impossible to exactly replicate the experimental results as well as it is difficult to subsequently suggest a computational model valid for a wider range of cell cultures.

As already mentioned, assessing the mechanical properties of individual components *in vivo* is particularly complicated and only a few to none sources introduce an experimental method that does not include separation of the component from the living cell body which, mainly due to rapid deterioration, induces a significant error [21]. The evaluation of the component behavior within the cell body is important due to the constantly changing dynamic nature of the inner arrangement [37, 41], which is disrupted by whichever separation.

Additionally, an indirect approach leading to a determination of mechanical properties, i.e. extracting the results of individual components from global cell response [34], introduces errors in the order of the value itself which needs to be accounted for when evaluating and utilizing such results. Preferably, an equilibrium between the level of uncertainty and a possibility of living cell disruption needs to be achieved in order to obtain viable results.

In Table 4.1, examples of mechanical properties available from literature focusing mainly on the elastic modulus of the three volume-significant components are demonstrated. Since numerous computational models estimating and evaluating the material properties are already available, the summary also includes such mechanical

properties herein perceived in a broader sense as material model parameters that appeared in one of the proposed models. All of the values are introduced in a unified manner as Young's modulus (some minor calculations may have been performed to unify the values), so the values can be subsequently directly applied for the following model definition.

The cytoskeletal components are commonly described as elastic isotropic homogeneous material due to the lack of detailed information about their individual behavior. Advantageously, the Neo-Hooke material model is often associated with continuous components since only two parameters (elastic modulus and Poisson's ratio) need to be assigned. The constitutive models suitable for cell mechanical behavior study will be discussed further in detail.

Nucleus	**Membrane**	**Cytoplasm**	**Source**
1–10	×	0.1–2.5	Caille [10]
1	10	0.25	Lebiš [34]
1	30	1	Holata [26]
8.25	7.5	3	Slomka [42]
5	1000	0.5	Bansod [3]

Table 4.1: A literature summary on elastic modulus values (in kPa) determined component-wisely. The data are organised according to their publication date. The values reported differ with calculation method (by a mere estimation and iterative verification or a more complex calculation). Refer to the source publications for more details.

Focusing additionally on the mechanical properties of the mitochondrial system, more publications need to be researched. As a way of example, the range 0.096–0.115 MPa is reported in [32] which is in an almost perfect agreement with the values reported recently by [28] increasing the range to 0.01–0.2 MPa.

Epithelial vs. endothelial cells

It needs to be noted that most of the research focuses on endothelial cells forming closed-type body systems [9]. The research performed at the Institute refers to cells of the blood circulatory system with atherosclerotic arterial wall [6] with the aim to understand the pathophysiology on a micro-level.

Nevertheless, all of the experimental data obtained from the Department of Pathophysiology research are extracted from human epithelial cells [38] and thus, the difference needs to be assessed. Epithelial cells can be found in tissues connected to the outer surroundings [9] such as skin but even the respiratory system, liver, kidney, and intestines. The cells of epithelium are tightly bound to each other as illustrated in Figure 4.1 which is in contradiction to the arrangement of endothelial cells that are surrounded by extracellular matrix, e.g. by collagen fibers. The closely-bound epithelial cells interact mainly with other cell bodies therefore their loading conditions are supposedly somehow different.

As for the particular evaluation of the difference between the mechanical properties of endo- or epithelial cells, other experimental studies agree with the validity of similar overall elastic moduli for both types of cells. To confirm this statement, mean values of whole-cell elastic modulus for the PC-3 (the abbreviation stands for prostate cancer)

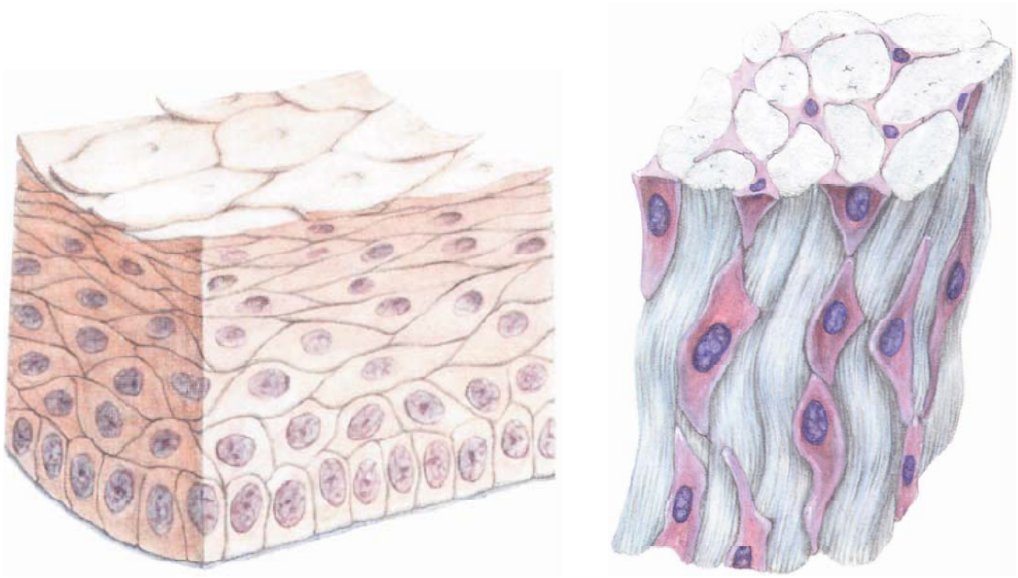

Figure 4.1: Left: Stratified epithelium formed by multiple layers of cells that can be found for example in mucous membranes, right: connective tissue with significant amount of inter-cellular matrix such as collagen fibers, adapted from [9].

cell line were established using a variety of experimental methods by the Department of Pathophysiology representing the epithelial cells:

1. AFM, pyramidal tip [38]
$$E = 1210\text{Pa}$$
2. AFM, spherical tip with radius 5 µm
$$E = 900\text{Pa}$$
3. real-time deformability cytometry
$$E = 925\text{Pa}$$

which is in good agreement with whole-cell modulus reported for example in [47], where the reported value "0.71±0.16 kPa in HUVEC and 0.94±0.06 kPa in SC cells" (both endothelial cell types). The higher value derived from sharp-tip indentation is observed and can be justified by the varying method resolution, different indentation depths (commonly higher values in pyramidal tip indentation [16]) and cell's interaction with different loading conditions (namely, the higher values of conical tip AFM are possibly explained by cell actin cortex behavior [47]). Note that the magnitude of whole-cell elastic modulus is of the same order as the modulus established for the cell nucleus (see Table 4.1). Since only a few sources aim at the comparison of the mechanical properties in the two types of cells, the difference will not be discussed further.

As the general base ground for computational modeling was summarized in sufficient detail, the different approaches utilizing those previously stated pieces of information will be presented further. The following sections aim at briefly introducing the computational models characterized by various levels of simplification of the inner cell structure (ranging from the simplest continuum-based models to sophisticated hybrid approaches) [2].

4.2. Continuum models

Continuum models can be characterized by incorporating only continuous components, i.e. the regularly distributed components that can be described using simplistic material models, linear or more frequently non-linear [34], most commonly homogeneous isotropic continuum assessing cell elasticity [25] or viscoelastic models for evaluating response to time-varying stimuli, e.g. creep [2, 30]. Generally, the continuum models serve for studying the macroscopic properties of the cell. The approximation of the cell components with the continuum approach enables two-dimensional axisymmetrical modeling and serves as an initial step for advanced modeling by identifying the basic parameters for further usage.

Those models can be divided further into structural and non-structural models [25]. Structural models are described in further detail in Section 4.2.1. Non-structural models aim at describing cell mechanical response by assigning only one material model to the whole cell body completely neglecting the inner arrangement and the reinforcing character of the cell components. Overall, the non-structural and structural model should be complementary, i.e. indicating the same stiffness when adjusted for the same experimental data. The continuum-based approaches available from literature are demonstrated in Figure 4.2, additional sources can be found in [2, 34, 33, 42]

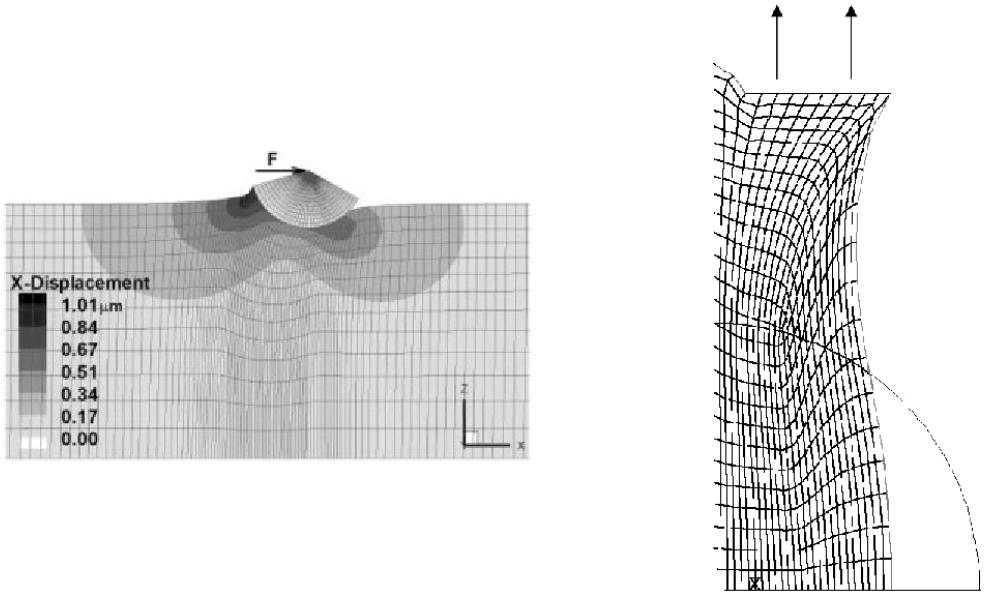

Figure 4.2: Continuum-based models introduced in literature. Left: a continuum model utilized for deriving viscoelastic response to magnetic twisting cytometry loading conditions [30], right: continuum simulation of tensile testing [34].

4.2.1. Heterogeneous models

Structural continuum models already incorporate some of the cell structural components (namely the cell nucleus, membrane, and cytoplasm can be classified as continuum components). Even though it can still be marked insufficient for advanced simulation, it provides fair initial results. An example of heterogeneous continuum-based modeling for assessing the cell heterogeneity in comparison with experimental data, namely AFM force maps, can be found in publication from Tang [46] (refer to Figure 4.3).

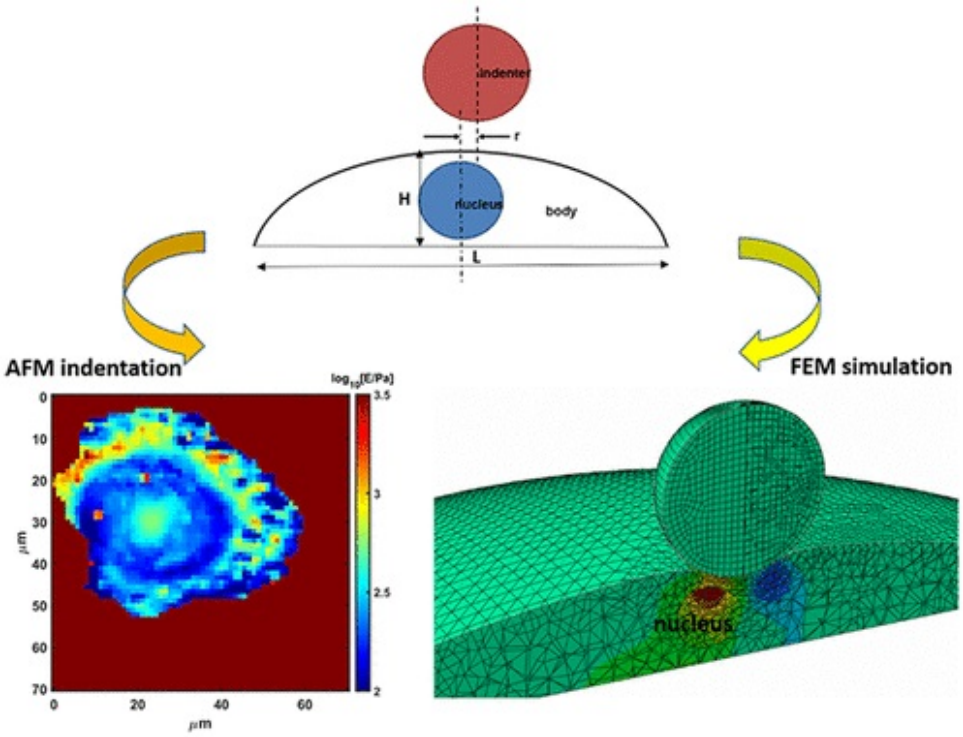

Figure 4.3: Evaluation of cell heterogeneity using a comparison between continuum-based heterogeneous model response with AFM force maps, adapted from [46].

A similar modeling approach is to be utilized in subsequent parts of the thesis to initial definition of the model geometry, validation, and adjustment of the material model parameters introduced in the literature overview.

4.3. Discrete compartments

Discrete element modeling is often used for including spaced, irregular components residing within the cell volume into the calculation. To be more specific, the discrete models describe the spatially irregular organelles mostly in the form of beams, trusses, or links with rope-like behavior. Such arrangement results in model heterogeneity [3] and thus describes the cell complex behavior in a more accurate manner than continuum-based models.

The specific structural arrangement that serves for maintaining the cell shape and is responsible for its stability is mainly generated specifically in cytoskeletal components. The details and definitions are introduced in the following section.

4.3.1. Tensegrity

Tensegrity (tensional integrity) defining the cell shape is a geometry structural arrangement, also more generally observed and utilized used phenomenon in solid mechanics, e.g. arrangements in civil engineering applications such as self-stabilizing bridges.

As the definitions and terminology vary with each author and depend namely on the field of application, it is to be noted, that even though other applications are certainly interesting, this section provides further details on 'biotensegrity', i.e. the tensegrity structures in living organisms [40].

The stability and self-supporting character of a tensegrity structure is based on the force equilibrium within the network of pre-stressed tension-only elements and compression elements which form a complex interconnected system that transfers loads applied to the structure [25, 34]. This is contradictory to classic mechanical arrangements, such as temple domes, where the stability is generated by continuous compression forces developed as a reaction to gravitational force [26].

The constituent elements can be differentiated by their character as tension-only elements and compression elements [18]:

1. **Tension-only elements**: a continuous pre-stressed web of cables transferring only tension, and

2. **Compression elements**: elements that are subjected to tension and compression and are not able to transfer loads between individual compression elements (they are connected just to tension-only elements).

The corresponding assignment of the cytoskeletal components with their tensegrity characteristics and function in context of the cell is enclosed below in Table 4.2 for clarification.

Cytoskeletal component	**Function**	**Tensegrity character**
Actin filaments	Reinforcing & movement	Tension-only
Microtubules	Transport	Compression
Intermediate filaments	Interconnecting & spatially stabilizing nucleus	None*

Table 4.2: Cytoskeletal components and their characteristics with respect to tensegrity structure [3, 26]. *Intermediate filaments are not a part of the tensegrity structure arrangement even thought they fulfill the reinforcing function of the cytoskeleton.

The tensegrity is often associated with important wording "continuous tension and discontinuous compression" [34] which characterizes the inner load distribution precisely as demonstrated in Figure 4.4. Another integral part of the tensegrity definition is the pre-stress. Generally, the stiffness of the structure almost linearly depends on the amount of pre-stress present [3] which is briefly demonstrated further in Section 5.3.

The tensegrity structure is generally capable of responding to local loading conditions on a global level. However, when the stability of the structural arrangement within a living cell is disrupted, it is capable of a reorganization (e.g. when subjected to varying loading conditions) and thus redistributes the load between the individual components to adapt to immediate loads.

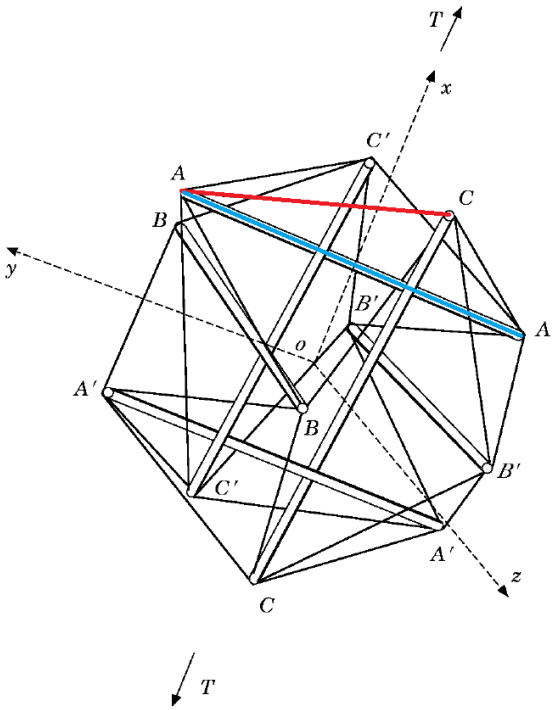

Figure 4.4: The basic tensegrity: six-strut structure as defined in [44], tension element highlighted by red, compression element in blue.

Apart from the material non-linearity (hyperelasticity) of continuous components, the linearly elastic discrete tensegrity structures present at the intracellular space are the main cause of cell non-linear behavior (usually referred to as geometrical non-linearity or generally strain stiffening observed during experimental cell testing [25]).

Bendotensegrity

While tensegrity structure generally incorporates straight bars or struts connected by ropes, fibers, or cables and its load response character is sufficient for initial cell computational models, bendotensegrity supplements the straight compression elements with bending (or flexural) load character, i.e. comprises of curved beams that are in equilibrium with their straight connections [3] which is in better agreement with inner structure reported in Section 2.1. Thus, bendotensegrity structures can be proclaimed a more precise approximation of the inner arrangement in the cell cytoskeleton, the difference between the arrangement in the straight-strut tensegrity model and bendotensegrity model is illustrated in Figure 4.5.

4.4. Hybrid models

It is advantageous to incorporate discrete elements into the previously established continuous model. The computational models incorporating continuous, as well as discrete elements, are commonly called hybrid models.

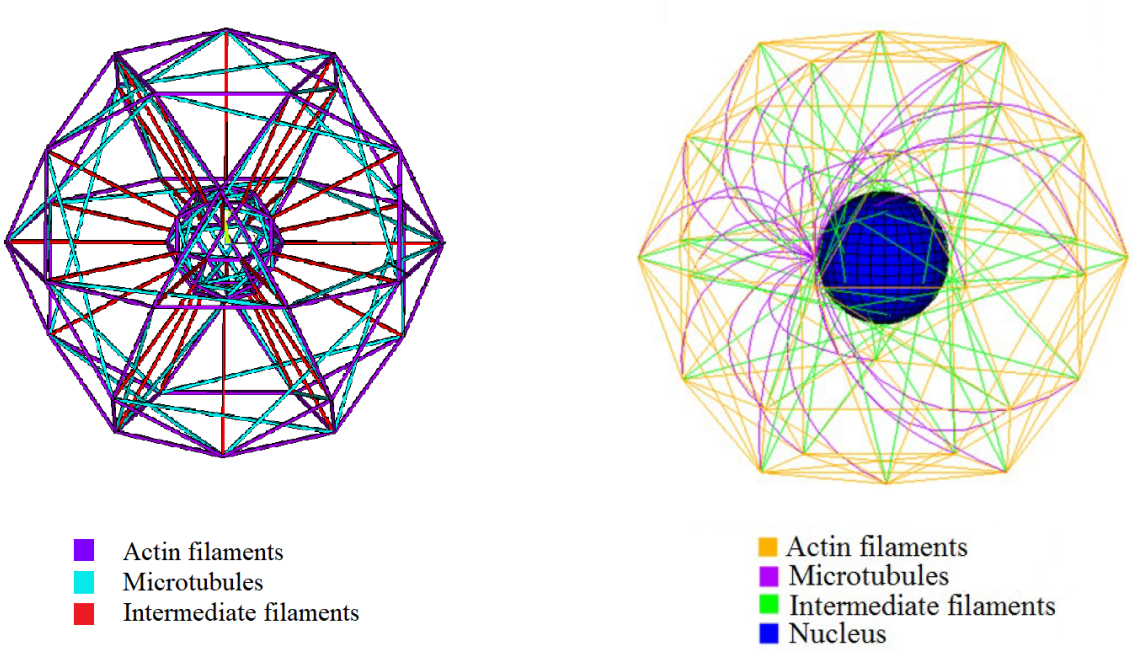

Figure 4.5: Comparison of tensegrity model form Bauer [5] incorporating inner nuclear cytoskeleton on the left with bendotensegrity model proposed in Bansod [3] on the right.

5. Multi-scale modeling

The model that is introduced in the following pages is being based on computational models proposed at BUT in previous years of dedication to the research that was briefly introduced above (see Chapter 4). Adopting all of the prior knowledge in the field and previously-made findings is an almost impossible task however the research bears a great potential when possibly combined into a comprehensive solution.

The new concept with the inclusion of mitochondrial network into the cancer cell structure has never been published before at the Institute of Solid Mechanics, Mechatronics and Biomechanics and its purpose is to evaluate the impact of mitochondrial system inclusion and its degree of coupling in the cytoplasmic volume on overall cell mechanics.

The cell structure and its properties are defined on a variety of experimental measurements of cells such as confocal microscopy (often in combination with fluorescence imaging) and the AFM indentation method. In cooperation with Dr. Gumulec at the Department of Pathophysiology the decision to perform a generalized assumption test on one culture of the cancer-affected cells has been made. Since the studied cancer cells extracted from human caucasian prostate adenocarcinoma are cultivated in an adherent state, only an adherent computational model is introduced herein in contrast with other research at the Institute, such as [3, 27, 34].

5.1. Input parameters

Comprehensive datasets concerned with the cell's inner structure as well as experimental measurements of its response have been provided. The novel concept is therefore being introduced with an aim to disrespect as few of the data-related facts as possible (e.g. the haphazard arrangement of the mitochondria, etc.) and the data are utilized as advantageously as possible.

5.1.1. Cell morphometry parametres

The cell morphometry parameters such as whole-cell height or nucleus shape dimensions (see Table 5.1) have been derived as a middle value from experimental measurements performed on hundreds of cells of the same prostate cancer cell line (PC-3) using tomographic or confocal microscopes. These dimensions are utilized further for the whole-cell model definition and as such, the volume is to be filled with mitochondria in particular. In future research, the volume of the cell could be gradually filled with whichever component, for example with cytoskeleton as identified in Section 4.1.

Whole cell dimensions [µm]	
Long axis a (xz plane)	40.4
Short axis b (xz plane)	20.3
Height c (y axis)	9.09
Nucleus dimensions [µm]	
Long axis a (xz plane)	16.7
Short axis b (xz plane)	10.6
Height c (y axis)	4.61
Actin cortex [µm]	
Thickness	0.270*

Table 5.1: Summary of the cell morphometry parametres for PC-3 cell culture, data obtained in collaboration with Department of Pathophysiology.

The membrane thickness presented in Table 5.1 was assessed using the thickness of the actin cortex (which, as already mentioned, is forming the membrane reinforcing endoskeleton and is responsible for what is called the cell membrane stiffness). Nonetheless, even the thicker actin cortex thickness is at the limit of the microscope resolution and provides no valuable information about the membrane thickness itself. For future reference, this parameter was set 0.1–1 µm according to the range available from literature [11] and supplemented with the membrane thickness 5–10 nm available from literature overview [3, 18].

5.1.2. Experimental force vs. indentation curve

Validation of the proposed computational model is to be performed by a comparison of the simulated force-indentation curve with an experimentally derived curve. The data sets are an invaluable contribution even for a future topic elaboration. Two data sets (partially published in [38]) have been provided by the Department of Pathophysiology on request. The round adherent cell shape of the PC-3 cells is advantageous for further implementation into the simplified cell model.

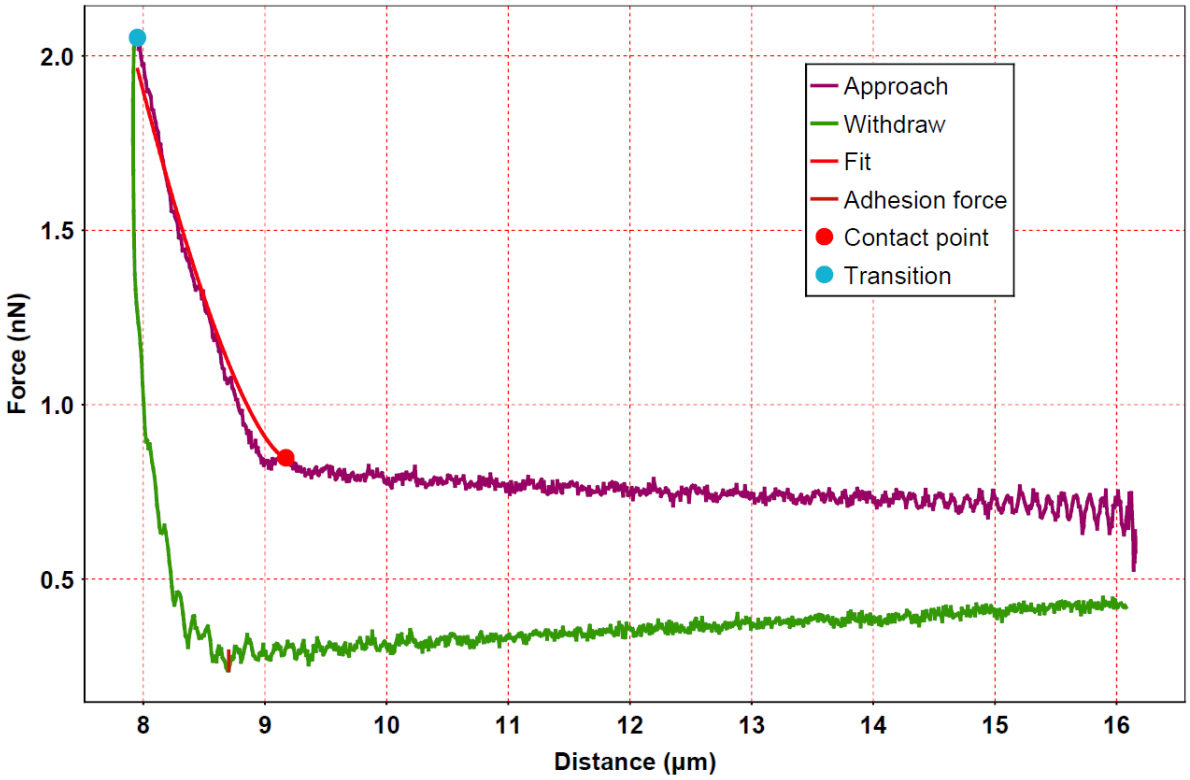

Figure 5.1: The recorded data from a single indentation point [24]. An approach phase (purple) and withdrawal (green) can be distinguished.

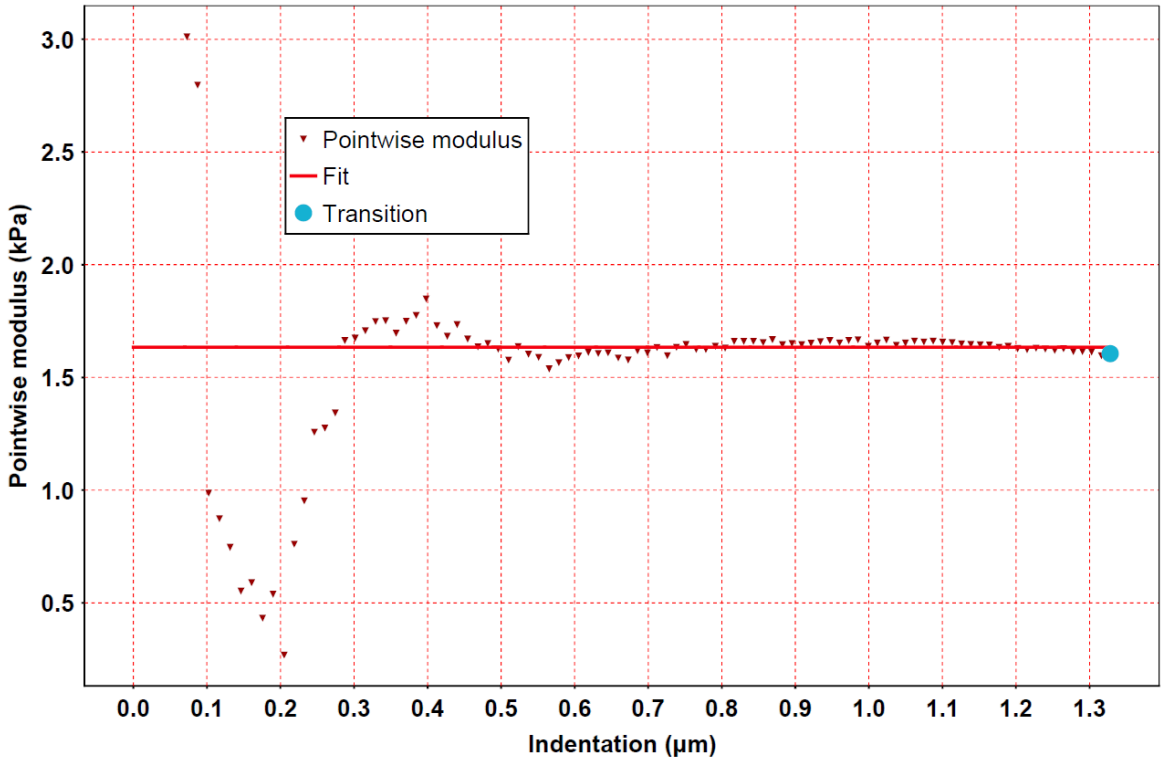

Figure 5.2: The point-wise modulus determined indirectly from the experimental data [24], resulting (mean) value is displayed in red.

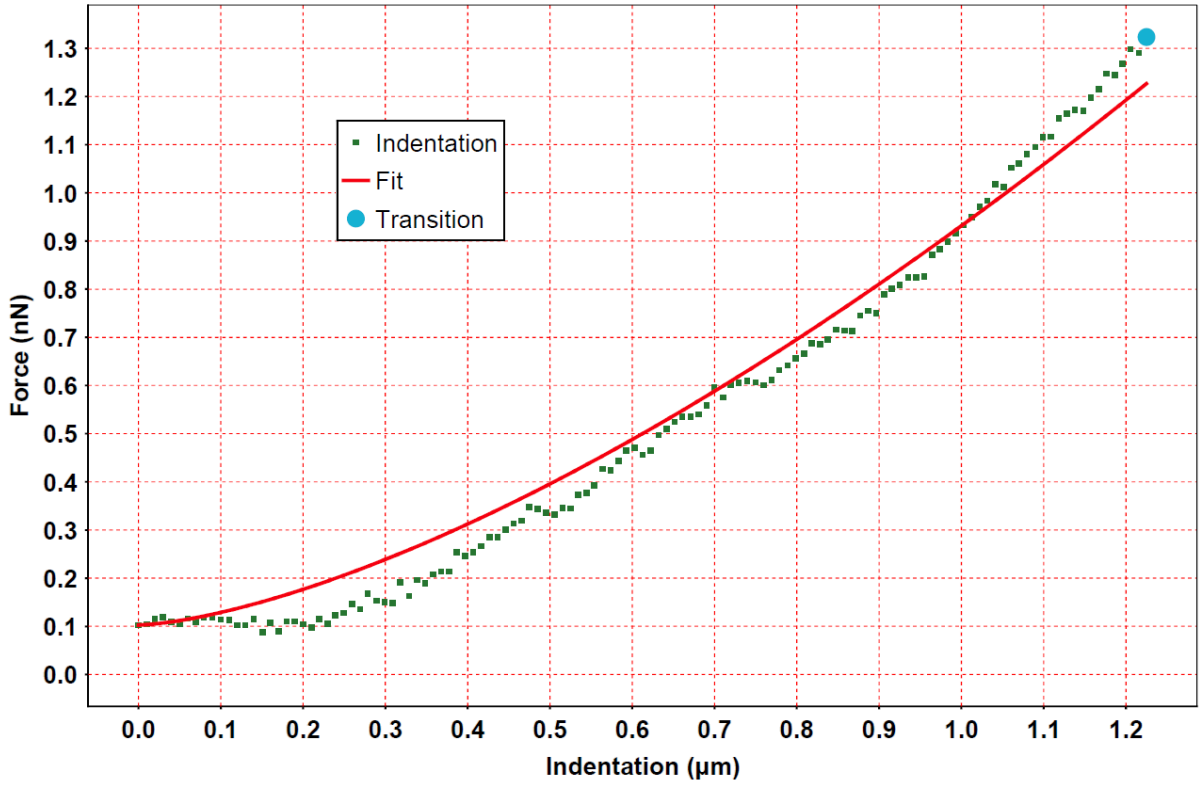

Figure 5.3: The raw data displayed as green dots and their interpolation (red curve) using the Derjaguin, Muller & Toporov (DMT) theory of adhesion in AtomicJ tool [24].

More advantageously, the data which are enclosed in Figure 5.1 do not need further processing other than the processing utilizing the integrated calculations built-in the AtomicJ tool, documented in [24]. The tool is dedicated to atomic force microscopy data evaluation and is capable of performing the approximation of the data and using a chosen methodology (such as DMT theory based on Hertz theory adjusted for spherical indenters and adherent-state cell on a rigid surface [1]), calculate the point-wise modulus (see Figure 5.2), and create various maps such as force map, etc. [24].

The interpolation may naturally result in the information loss as is apparent in Figure 5.3, where the interpolated curve corresponds with the overall cell stiffness, however, the information about the underlying structures is lost (can be observed as the waviness of the indentation data).

5.1.3. Material properties estimation

Due to the lack of experimental data available on the mechanical properties such as elastic modulus E, Poisson's ratio μ or shear modulus G of individual cell components of the PC-3 culture, the input data need to be supplemented by values from the literature overview (see Tables 5.2 and 5.3) where the most recent publications originating at the Institute [3, 27] serve as the main reference (see Section 4.1.2). In agreement with those models, discrete elements were considered an isotropic linear elastic material, and Neo-Hookean material is being assigned to the continuous elements [3]. As most of the sources incline towards Poisson's ratio equal to 0.5, the compressibility factor is not included as the indentation depths do not reach the level of compressibility having a significant

impact on cell behavior. This additionally means that the mixed u-P formulation (pure displacement) is used in all of the simulations.

Cell component	**Elastic modulus E [MPa]**	**Shear modulus G [MPa]**
Plasma membrane	1.0	0.33
Nucleus	5.0×10^{-3}	1.7×10^{-3}
Cytoplasm	5.0×10^{-4}	1.7×10^{-4}

Table 5.2: Initial estimation of hyperelastic properties of continuous components based on the literature overview [3, 10]. All of the components are considered incompressible, therefore the Poisson's ratio μ= 0.5.

Cell component	**Elastic modulus E [MPa]**
Actin filaments	2.60×10^{3}
Microtubules	1.20×10^{3}
Intermediate filaments	7.60
Mitochondria	0.100

Table 5.3: Estimation of elastic properties of discrete elements based on the literature overview. Parameters of cytoskeletal components adapted mainly from [3, 10], mitochondrial elastic modulus reported in [28, 32].

5.2. Continuum-based approach

Even though the cell as a whole unit is heterogeneous, some of its components can be described as homogeneous isotropic hyperelastic continuum [3]. This knowledge is advantageously utilized for continuum-components-only model preparation aiming at determining the material model parameters to be used for hybrid modeling (discrete elements incorporated into the cytoplasmic volume).

The main advantage of the continuum-based approach is the time efficiency and fast adjustment of the model (the computation time does not usually exceed minutes), meaning it is the perfect environment for material parameters estimation, even though the transition to a three-dimensional space introduces deviations from the computed response (illustrated in further details in Figure 5.7).

5.2.1. AFM indentation simulation (axisymmetry)

A two-dimensional model has been created primarily for the purpose of the initial material parameters estimation for various constitutive material models. Since the material behavior of every biological tissue is characterized by significant strain stiffening, more complex models are also considered and evaluated further. This initial simulation also serves as a validation of the mechanical properties found in sources and their adaptation for this particular case (adjustment for the particular data set).

The morphometry parameters from Table 5.1 were reduced for axial asymmetric calculation as follows in the Table 5.4. The sphere segment was selected to represent the simplified adherent cell shape (similarly to most of the studies dedicated to adherent cell

simulations). The idealized nucleus shape of the adherent cell is considered to be an ellipsoid with equal axes in the horizontal plane (the average value is selected as a representation with reference to the morphometry data).

Whole cell dimensions [µm]	
Diameter	30.37
Height	9.09
Nucleus dimensions [µm]	
Axis on xz plane (a = b)	13.64
Height c (y axis)	4.61
Membrane [µm]	
Thickness	0.01*
Thickness replaced with value form literature overview.	

Table 5.4: Reduced dimensions from Table 5.1 for axial symmetric model.

Even though the cell shape is generally described as spherical [26], it is highly adaptable. The cell shape depends on its surroundings: the presence of adjacent cells, its growing conditions (or even the conditions of its cultivation), and component arrangement within the cell body. The irregular shape is illustrated using confocal microscopy images (see Figure 5.4) and its shape variability could have been assessed using an automatized image processing. However, the simplified sphere segment shape is considered a sufficient substitution for reaching the goals defined at the beginning of the thesis. The solution can be therefore generally categorized as a separate cell assessment (the cell is isolated from its surroundings).

The finite element simulation of the AFM test is to be established as a contact problem. The AFM tips vary in shape (as pointed out in Section 3.1) and the data sets available included spherical and conical indentors. This implies, that simulating the AFM indentation using the finite element method can be performed using both of the indenter types (as outlined in Figures 5.5 and 5.6).

The conical tip is suitable and even advantageous for initial material property estimation as herein, especially when the task is adjusted for axial symmetric simulation with contact modeling being replaced by simple one-point loading (boundary) condition.

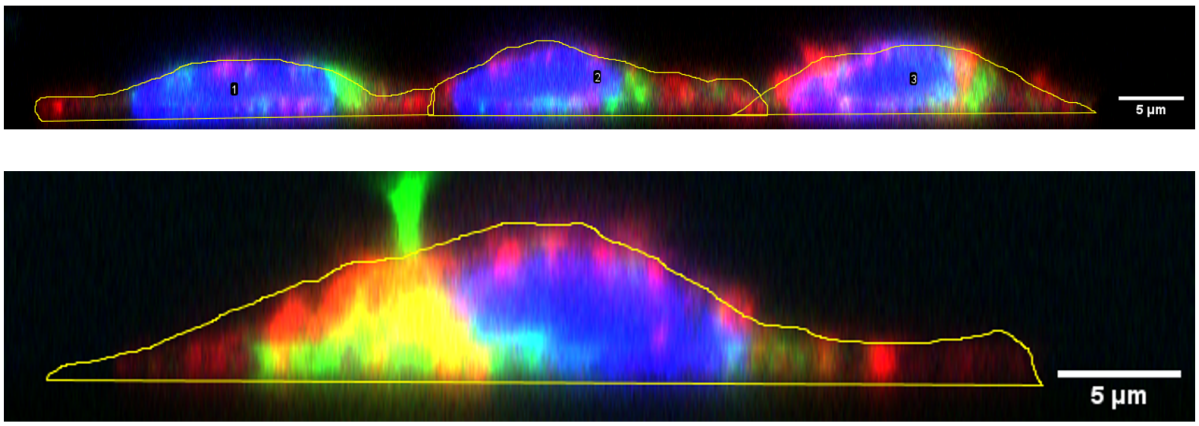

Figure 5.4: An actual shape of the cell body.

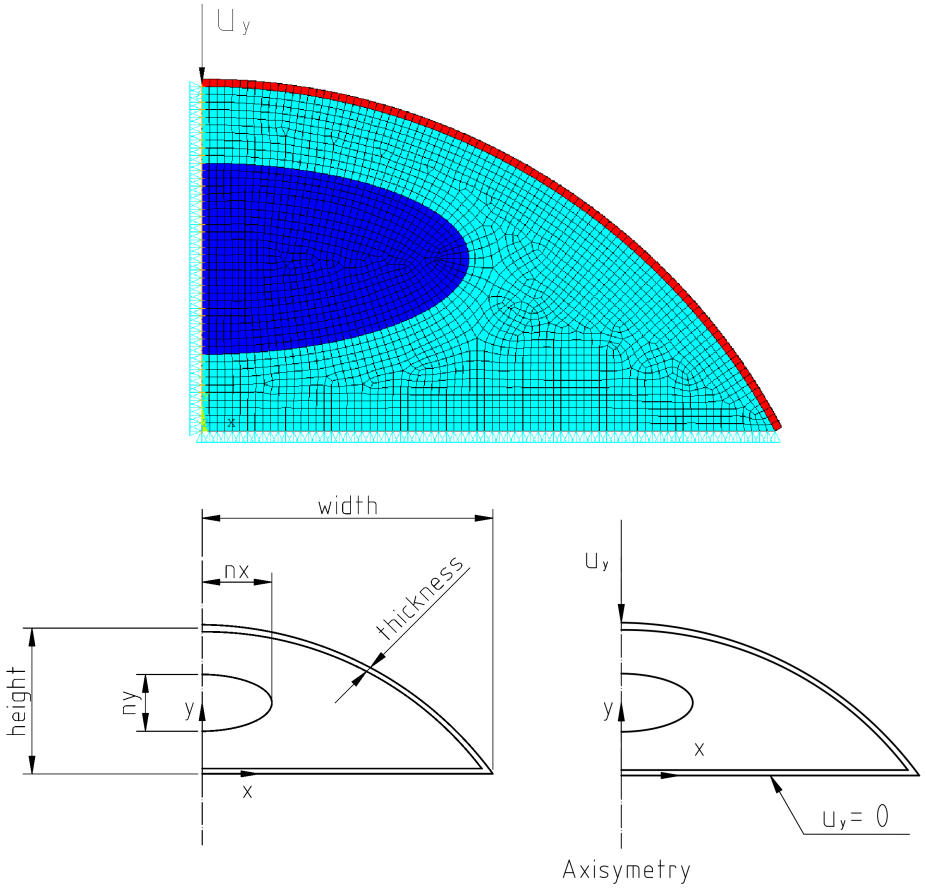

Figure 5.5: Top: the axisymmetrical simulation discretization: (red) cell membrane, (blue) nucleus and (magenta) cytoplasm. Bottom: boundary conditions and geometry outline for continuum-based approach.

However pyramidal tip geometry could potentially result in convergency issues in the three-dimensional problem solution. The cause is identified to be large local deformations when compared to cell dimensions (generally, the pyramidal indentation is of larger magnitude than the magnitude of spherical tip application) and more importantly step-change contact character caused by the tip geometry. Therefore, as the solution subsequently transitions from plane axisymmetry into a highly irregular (heterogeneous) three-dimensional form, only the conclusions about the material properties derived herein will be utilized further. The Table 5.5 summarizes the element type selected to represent the heterogeneous continuous elements.

Cell component	**Element type**	**Property**
Nucleus	PLANE182	KEYOPT(3) = 1 (axisymmetry)
Plasma membrane	SHELL208 (axisymmetry)	Thickness 0.01 µm
Cytoplasm	PLANE182	KEYOPT(3) = 1 (axisymmetry)

Table 5.5: Element type assignment for two-dimensional continuum-based approach.

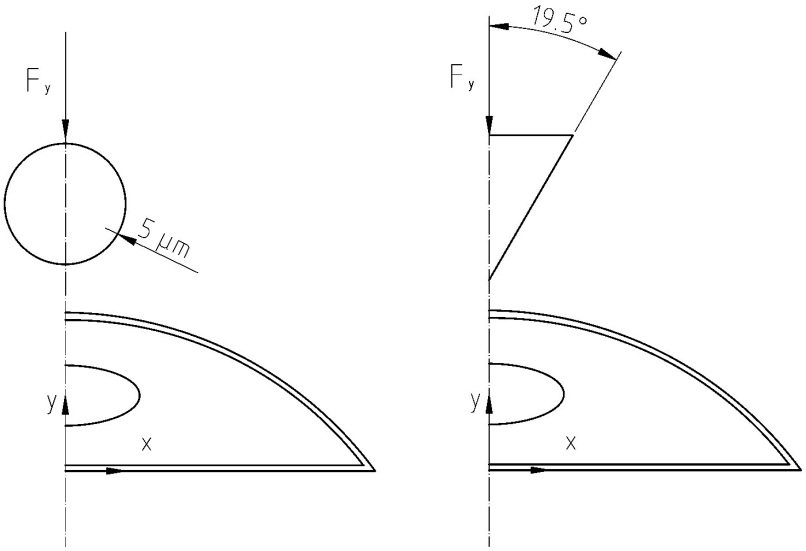

Figure 5.6: General AFM simulation outline with spherical and conical indentor.

5.2.2. Adjustment of the parameters

The first simulation respecting the initial shear modulus estimation implies, that the studied cancer cell line has lower stiffness than those of the previously presented models by [3, 27] which is in concordance with the research [21, 38]. Therein, the cancer is reportedly affecting the cell stiffness as is illustrated by the comparison of the simulated curve with experimental data fit in Figure 5.7 and the mechanical properties of the model need to be adjusted.

The difference between the experimental measurement and the simulated curve is to be enhanced even more when the dimensionality of the problem increases and the sharp tip is replaced by a sphere (as additionally illustrated in Figure 5.7). While the deviation

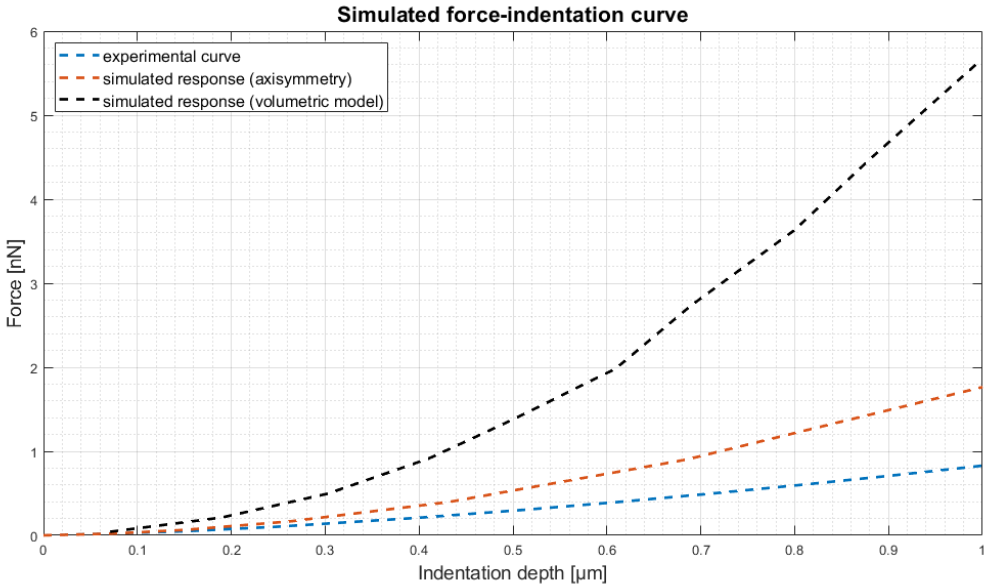

Figure 5.7: Comparison of reaction force determined computationally with experimental data whereas utilizing the initial estimation of mechanical properties (not adjusted for the particular data set).

observed when comparing the response of the axisymmetrical model is equal to double the anticipated (experimental) value, the observed force response in the volumetric model (described in the following sections) is approximately five to six times higher than the reaction force measured in live cancer cell culture.

Manipulation of material parameters (while preserving the geometry parameters) following the previously stated findings is carried out to calibrate the model for further calculations. A brief sensitivity analysis is included in Figure 5.8, where all of the initial shear modulus values varied as 50% 100% and 200% of the initially estimated value (as for example in [34]). Note that only the material parameters are subjected to adjustment due to the uncertainty of their determination in relation to the particular cell culture.

Following the sensitivity analysis which bears similar results to publications [3, 34], the model adjustment is susceptible to large deviations from reality when the membrane parameters are established incorrectly. Complying with the sensitivity analysis (as the desirable adjustment of the model is an iterative process and the deviations from the initial estimation need to be properly justified). All of the material parameters of the continuous components were gradually adjusted to half of the initially estimated value. Besides, as the response is highly sensitive to alterations in cytoplasmic shear modulus (in comparison with adjustment of nucleus parameters), it was decreased to 1/4 of the initial value to reach the results of the experimentally determined response curve. Lowering the shear modulus of the cytoplasm beyond other mechanical properties of the continuous approach is implied by mitochondria occupying a larger volume than the cytoskeleton for which the initial values of shear modulus were evaluated [3].

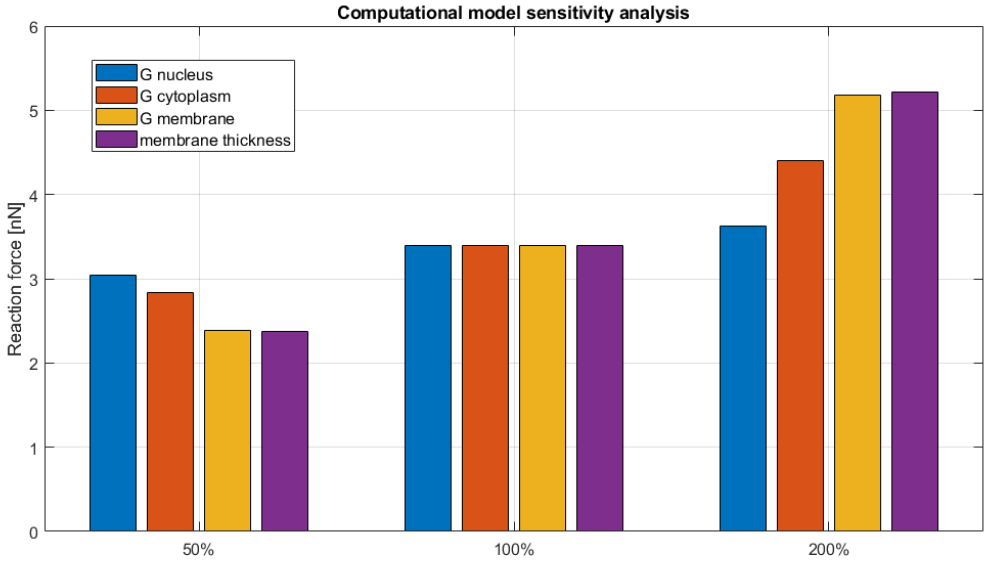

Figure 5.8: Sensitivity to the variation of selected parameters of the computational model. Assessed through a response of the model to indentation 1.2 micrometers.

5.2.3. Alternative constitutive models

Following the researched information summarized in Section 5.1 usually the Neo-Hooke constitutive material is being prescribed. However, the absence of a strain-dependent stiffening effect can be considered crucial for underestimating the mechanical response.

The shape of the reaction force curve reportedly showing strain stiffening associated mainly with cytoskeleton deformation (which is not being included in the proposed model) can be improved by incorporating Arruda-Boyce or Yeoh (3-parametric) material model. The constitutive models are being selected from a group of hyperelastic models even though viscoelasticity could have also been considered especially for viscous cytoplasm as in [30]. Note that the largest strain occurs at the membrane layer, therefore the constitutive models will be advantageously altered there, other components are not deformed to such extent therefore their larger non-linearity is not expressed and the strain-stiffening effect is negligible.

Neo-Hooke material model

The Neo-Hooke material model provides the advantage to utilize only one or two parameters to completely define the material model. The parameters to be defined are presented in the strain energy density function formula (with conventional designation for the tensors):

$$W = \frac{G}{2}(\bar{I}_1 - 3) + \frac{1}{d}(J-1)^2$$

where G represents an initial shear modulus and d stands for material compressibility (neglected in the proposed model). The parameters suitable for the particular case description are already evaluated in Tables 5.2 and 5.3 above.

Arruda-Boyce material model

Arruda-Boyce material representation belongs to a group of structural material models with defined physical nature of its parameters. In this case, in addition to the Neo-Hooke parameters, λ representing limiting network stretch is estimated larger than one (approximately 1.2 as in Figure 5.9) to induce sufficient strain-stiffening effect to the cell response.

Third order Yeoh material model

Inducing the strain stiffening (while the cytoskeleton is absent) can be performed by assigning higher order polynomial models. In this case, the three-parametric Yeoh model is selected to represent the polynomial class of constitutive models.

Strain energy density function formula of the material model based on Mooney-Rivlin formulation [7] is as follows:

$$W = c_{10}(I_1 - 3) + c_{20}(I_1 - 3)^2 + c_{30}(I_1 - 3)^3$$

with the parameters selected to approximately correspond to the Arruda-Boyce model described above are in the Table 5.6. Manipulation with the amount of the strain stiffening can be performed by adjusting the constant c_{30} which has been estimated from 0.08 (low impact) up to 0.2 depending on the approximated data.

c_{10}	c_{20}	c_{30}
0.221	0.0463	0.0837

Table 5.6: Constants of the three-parametric Yeoh material model.

The graphic representation is attached in Figure 5.9 to demonstrate the impact of substituting the Neo-Hooke model with another constitutive model on the resulting force-indentation curve. As it seems that more complex material models comply with strain stiffening conditions better (substantial in the steeper experimental curve), it has been still opted for the Neo-Hooke constitutive model for further proceedings based on insufficient knowledge about the individual material behavior while subjected to biaxial or shear loading. Besides, this material constitutive model should be capable of providing satisfactory stress results and even the response curve shows a satisfactory slope.

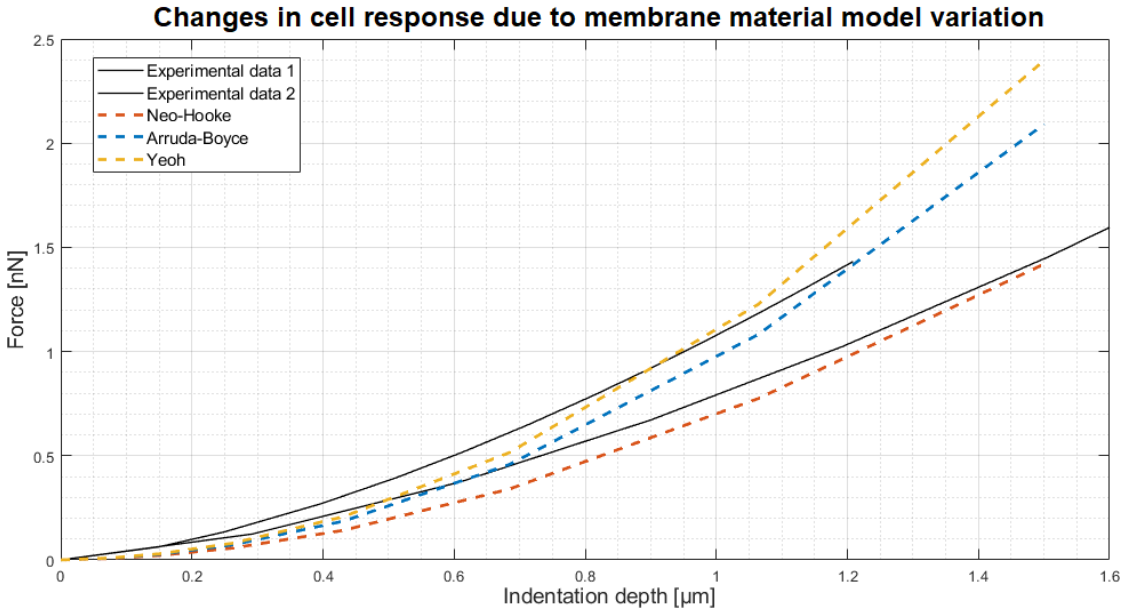

Figure 5.9: Depiction of a response to membrane constitutive models variation in comparison with experimental data.

5.3. Discrete elements: Tensegrity

Although a bendotensegrity model of cytoskeleton was assumed in the original formulation of the thesis, collaboration with MUNI brought a completely new focus to this problem. The idea of significant mitochondrial contribution to the overall cell stiffness became a basis of a new scientific project proposal, and some preliminary assessment of the role of the mitochondrial network was needed. Therefore a different composition of the model is being applied, with a realistic mitochondrial network within cancer cells and without a specific structure representing cytoskeleton (see also Section 4.1.1).

Nonetheless, to comply with the Goals defined in the Assignment, I would like to introduce a methodology for modeling tensegrity structures within a cell unit. The

purpose of this chapter is solely to clarify the cell behavior induced by cytoskeletal components.

5.3.1. Pre-stressed cytoskeletal components

The adherent state model introduced in [3] incorporates microtubules, intermediate filaments as well as actin filaments. As presented multiple times, the fibers differ mainly with the internal state (when the whole cell is characterized as *at rest*). Internal pre-stress is the main property of all the actin filaments and as a result, they appear straight at all times. On the contrary, intermediate filaments are commonly wavy and engage only at certain deformation levels. Both actin filaments and intermediate filaments act as cables, i.e. if under compression, the internal stress equals zero (for tension-only LINK elements, the option SECCONTROL = 1 is assigned). This setting is demonstrated on Figure 5.10 and supplemented by definition of individual filaments for FEM calculations in Table 5.7.

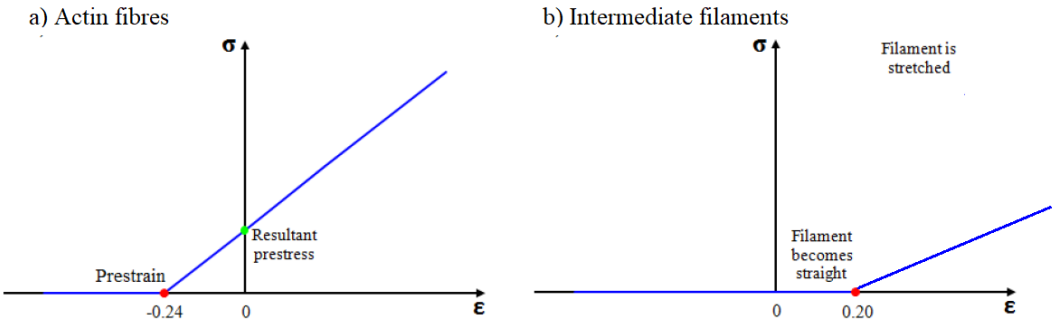

Figure 5.10: Illustration of the stress-strain behavior of actin fibres and intermediate filaments. The different slope is caused by the difference in the reported elastic modulus of individual fibers, adapted from [3].

Cell component	Element type	Property
Continuous elements		
Nucleus	SOLID185	
Plasma membrane	SHELL181	thickness 0.01 µm
Cytoplasm	SOLID185	
Discrete elements		
Actin fibres (AFs)	LINK180	⌀ 7 nm tension-only (positive pre-stress)
Intermediate filaments (IFs)	LINK180	⌀ 10 nm tension-only (negative pre-stress)
Mirotubules (MTs)	BEAM188	circular tube OD 25 nm ID 17 nm

Table 5.7: Element type assignment for tensegrity modeling, discrete elements representing cell cytoskeleton, adapted from [3].

The preliminary stress-strain curve of both actin filaments and intermediate filaments is demonstrated on a tensegrity arc geometry, where a) actin filament acts as a pre-stressed bowstring (the value of pre-stress was derived by measuring pre-strain in separated actin bundles [14]) and b) intermediate filament is relaxed until a certain level of deformation (approximately at 20% elongation [49]). A microtubule acts as the bow's body in both cases, the outline is illustrated in Figure 5.11. Once again, the values of elastic modulus differ through the sources, so they are adapted from the Institute's most recent publications dealing with tensegrity [3, 27] and thus are to be defined as $E = 2600$ MPa for actin filaments and $E = 7.6$ MPa for intermediate filaments. The prestress values therefore correspond to $\sigma_{AFinitial} = 620$ MPa in actin fibers and $\sigma_{IFinitial} = -1.5$ MPa for intermediate filaments.

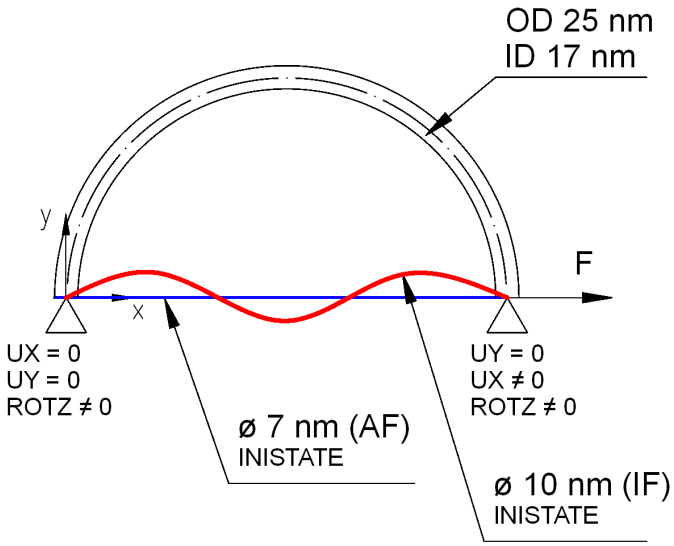

Figure 5.11: Outline of the tensegrity arc evaluation with the boundary conditions created for response assessment.

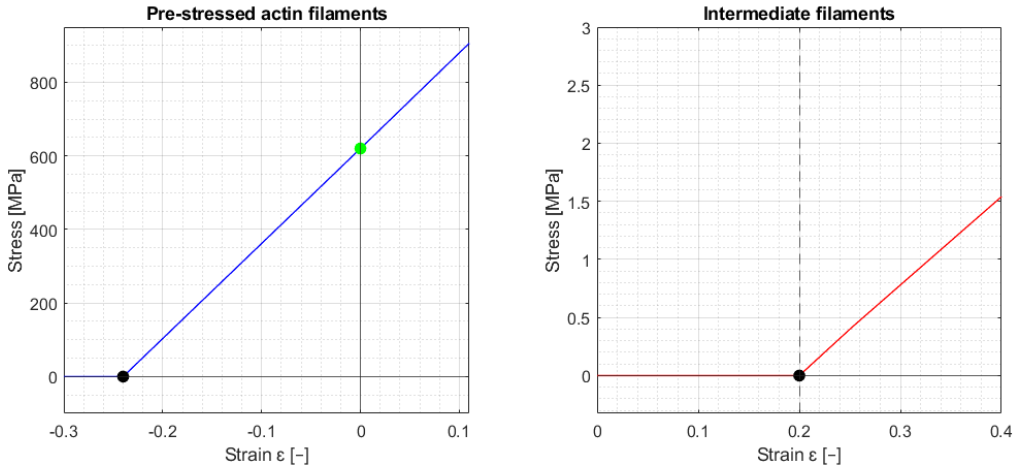

Figure 5.12: The simulated response of actin fibers with non-zero stress at zero deformation highlighted in green (left) and intermediate filaments engaging only after a certain amount of deformation (right). The characteristic behavior to be observed especially at the marked points. Note that the axes are not equal and the slope is distinguishably steeper in actin fibers than intermediate filaments.

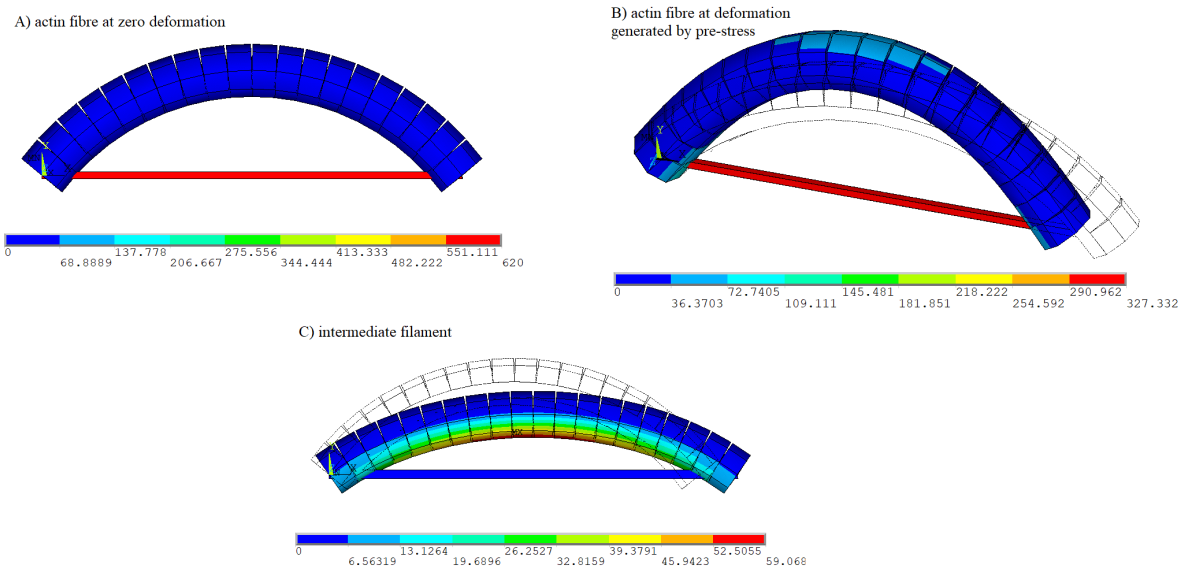

Figure 5.13: First principal stress distribution in the two types of filaments (acting as a bowstring embedded into a microtubule) with its own characteristic behavior A) pre-stressed actin fiber at zero deformation, B) deformed shape induced solely by the pre-stress, and C) intermediate filament showing zero stress even after deformation of approximately 10% of the filament length is induced.

The application of previously described initial conditions can be defined using the INISTATE command, assigning the corresponding value of initial stress, for example, according to the material number. The results of the stress state under zero deformation correspond with the assigned condition, i.e. actin fibers already show substantial stress and intermediate filaments remain unstressed. Both described cases are illustrated in Figures 5.12 and 5.13.

Note, that it has also been reported, that the higher the pre-stress in the network, the higher the system's stiffness. This is corroborated by deriving the reaction force

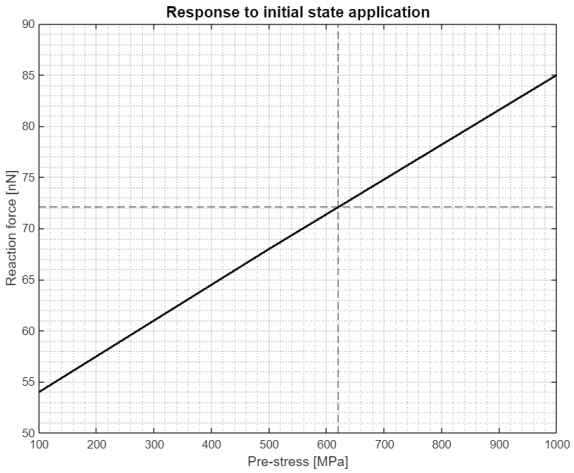

Figure 5.14: A linear dependency between the stiffness (reaction force magnitude) and the pre-stress introduced to the tensegrity arc. The dashed lines highlight the actual pre-stress value corresponding to actin fibers initial stress.

generated by the pre-stress induced to the arrangement, see Figure 5.14 which shows that this dependency has a linear character for a single fiber however a non-linearity in the response appears while multiple fibers combine.

As the cytoskeletal system is not included in the proposed model, it also needs to be noted that such neglect (or rather not-inclusion) results in reaction force decreasing by approximately 30% to 40% [3] which needs to be taken into consideration for further proceedings, i.e. the true initial shear of cytoplasm defined in the presented model would correspond to lower values if ever to be adjusted for the inclusion of the cytoskeleton.

5.4. Mitochondrial system inclusion

The proposed model does not include tensegrity structures, however, the beam-like structures are still a viable representation even for the mitochondrial system that is going to be evaluated herein.

The realistic morphology of the mitochondrial system is an inseparable part of the proposed model. The advantage of the mitochondrial network in comparison with the cytoskeleton is that thanks to the mitochondrion's larger diameter, it is possible to rather easily automate the scanning procedure. The subsequent processing of mitochondrial geometry, in preparation for the incorporation into the computational model, is assessed in a number of steps aiming at simplifying the complex morphology in a controlled manner:

1. Confocal microscopy 3D images extraction (supplied by Department of Pathophysiology);
2. Surface model creation based on those 3D images;
3. Mitochondrial network assessment in MitoGraph tool [23] which interpolates the complex surface mitochondrial geometry with nodes and its connections thus creating an interconnected system of lines and nodes; and
4. Simplification of the acquired line model using a Python script:
    - Overall dimensions adjustment for intended whole-cell sphere segment shape (see Figure 5.15); and
    - Complex mitochondrial skeleton geometry replacement with 3-point arc geometry (inducing constant curvature along the line) and small segments removal (or rather quantity of mitochondria being controlled).

As the mitochondrial system scanned using a confocal microscope is highly irregular, the impact of geometry adjustments (designed to compensate for such haphazard nature of the arrangement) described in the following paragraphs will be considered negligible when compared to other possible inaccuracies of the proposed model. The main irregularities lay in an irregular mitochondrial distribution in the cytoplasmic volume, the individual mitochondrion non-uniform thickness as well as the variable curvature along its mid-line which is assessed in point 4 of the above-defined list.

To begin with, the adjustment of the overall dimensions can be performed as outlined in Figure 5.15 below, whereas A) represents the circular area near nucleus surroundings with the highest mitochondrial density, B) represents elliptic area containing most of

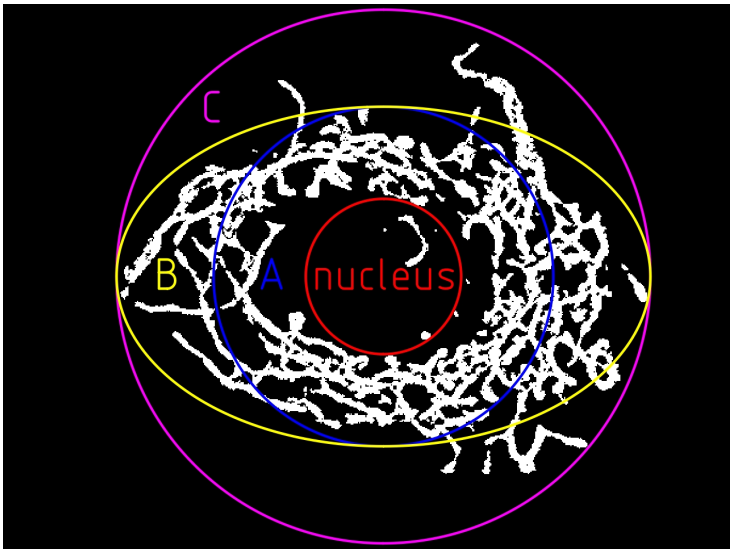

Figure 5.15: Whole-cell shape approximation possibilities demonstrated on an overall PC-3 mitochondrial system image (top view).

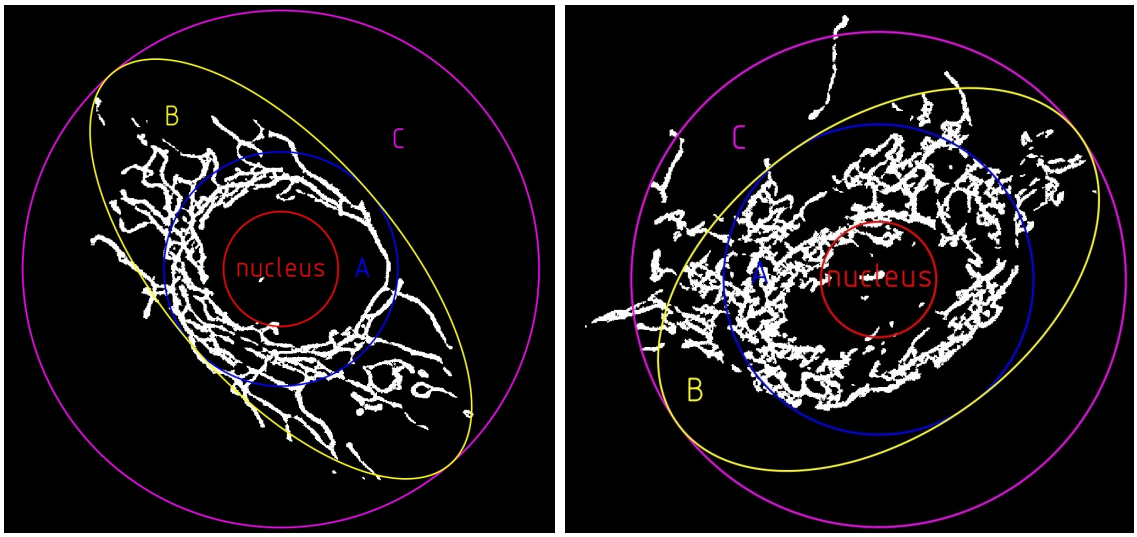

Figure 5.16: Additional shape approximation possibilities demonstration.

the mitochondria, and C) represents circular area circumscribing all of the mitochondrial structures (with maximum diameter). As illustrated, it is insufficient to include only the area which is filled with mitochondria since it results in neglecting a significant part of the mitochondrial system. It is also apparent from the figure, that the ellipsoid segment could have been selected as a whole-cell shape representation, however, this may be valid only for certain cell cultures (not universally), therefore, a more general shape C was opted for. Two additional examples of similar approximation on the PC-3 cell culture are attached in Figure 5.16 to illustrate the universal character of the herein proposed whole-cell shape approximation.

The mitochondrial skeleton (i.e. the lines connecting the junctions within the mitochondrial system) geometry replacement was deemed necessary due to the complexity of the structure illustrated in the previous paragraphs, the possibilities of the replacement that were at least considered (not always implemented further) are illustrated in Figure 5.17.

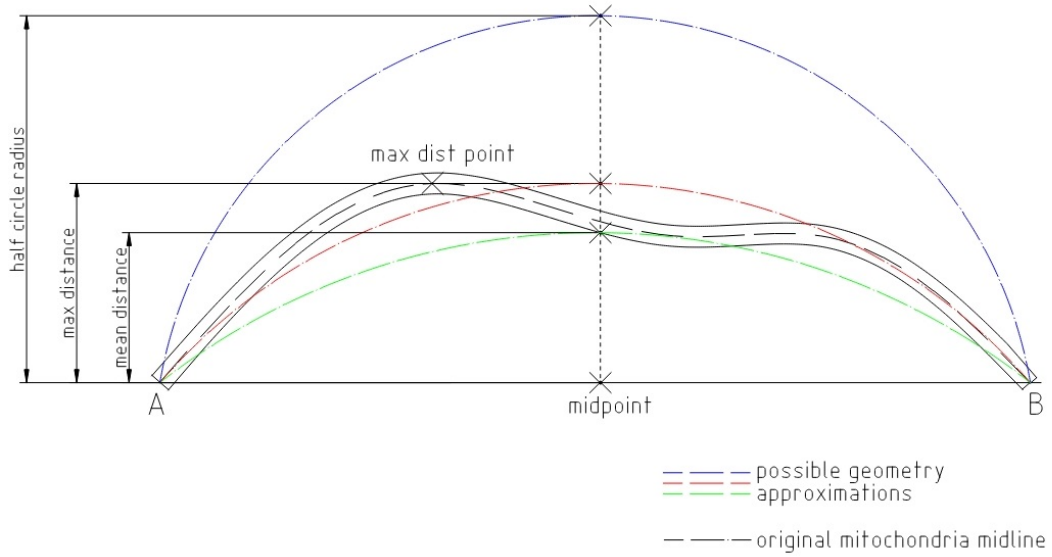

Figure 5.17: Possible mitochondrial geometry replacements with curved beam elements (replacing complex spline geometry with beams of constant curvature along the line).

The selected *max dist point* option investigates the individual lines of the model generated by the MitoGraph tool, finds a point of the largest distance value from the line connecting its first and last point, and assigns that distance to the midpoint of the arc (perpendicularly to the connecting line). This method utilizes all of the data from MitoGraph and the replacement is considered to capture the curvature impact on the stiffness in the best possible way. The final visualization of the mitochondrial system (and the mitochondrial distribution along the y axis) prepared this way for subsequent FEM calculations is attached in Figure 5.18 and additionally as a top-side view in comparison with the original (real) configuration in Figure 5.19.

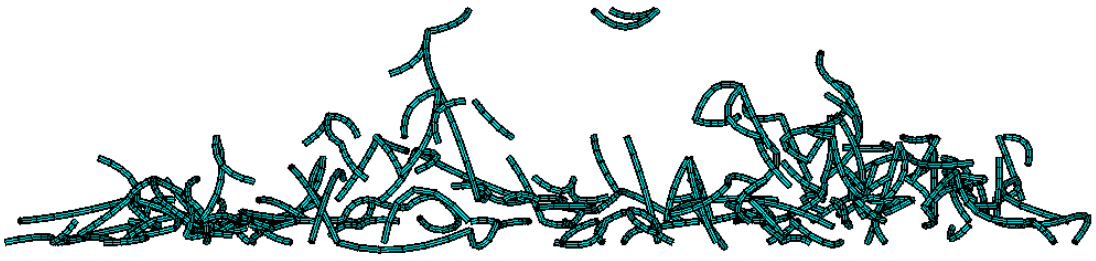

Figure 5.18: Side view visualisation of the simplified mitochondrial system (generated using the *max dist point* option) from Figure 5.15.

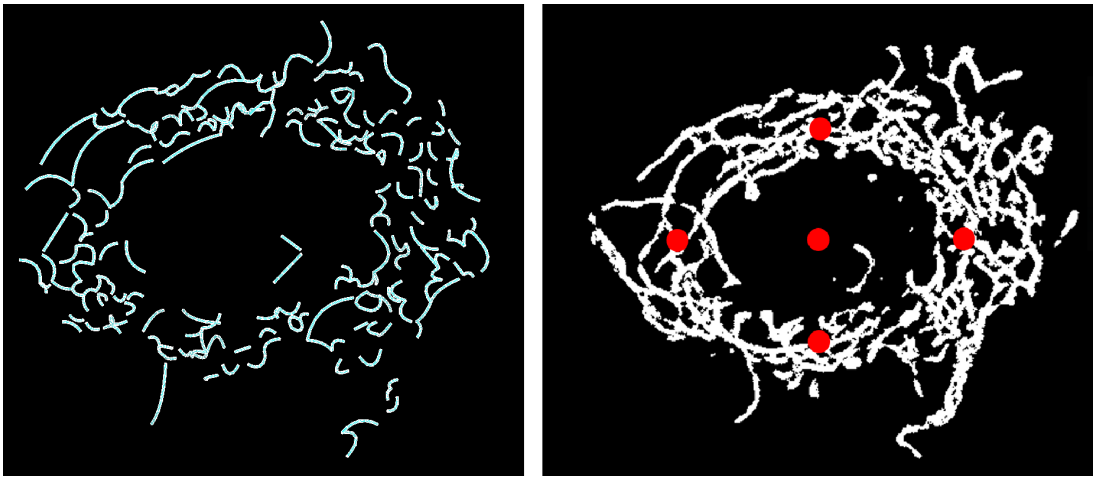

Figure 5.19: Comparison of the simplified geometry (left) using the *max dist point* option with the thresholded fluorescence microscopy image (right).

5.5. Interconnected model

As the presented individual continuous and discrete submodels combine, further analysis demands a transition from a two-dimensional continuum single point displacement approach to a more comprehensive three-dimensional contact problem solution. Contact incorporation introduces another non-linearity into the computation, however, it was deemed necessary for results viability.

The continuous model introduced in Section 5.2 was swept along the corresponding axis to generate a volume mesh, and the mitochondrial system either in a complex uniform-thickness or simplified shape was incorporated to reach the final hybrid model (refer to Figures 5.20 and 5.21). The element type designation for this calculation is presented in Table 5.8.

Cell component	**Element type**	**Property**
Nucleus	SOLID185	
Plasma membrane	SHELL181	Thickness 0.01 µm
Cytoplasm	SOLID185	
Mitochondria	BEAM188	Circular cross section Radius 0.234 µm
Indentation tip	TARGE170	Rigid body, frictionless
Contact elements	CONTA173	

Table 5.8: Element type assignment for hybrid modeling, note the addition of discrete elements representing mitochondria, modified from [3].

A general outline of AFM simulation is illustrated in Figures 5.21 and 5.22. Solely as an example, the separated areas of Figure 5.22 (allocated several micrometers below the top-point) are covered with contact elements CONT173 and the sphere indenter is an undeformable rigid body encased in TARGE170 elements, its degrees of freedom constrained to one pilot node at the center of the sphere. The rigid body approach needs to be naturally selected due to the stiffness value of the indenter exceeding the cell stiffness by eight orders of magnitude. Moreover, it is an advantageous choice as the boundary conditions prescribed for the pilot node will result in simultaneous movement

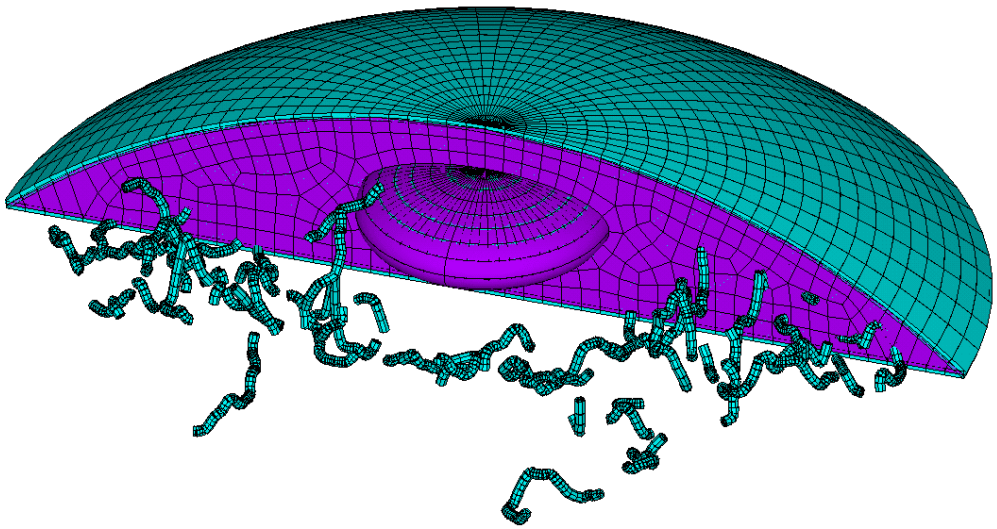

Figure 5.20: A pseudo-slice view of the complete (i.e. not simplified) mitochondrial system inclusion into the continuum-based approach model.

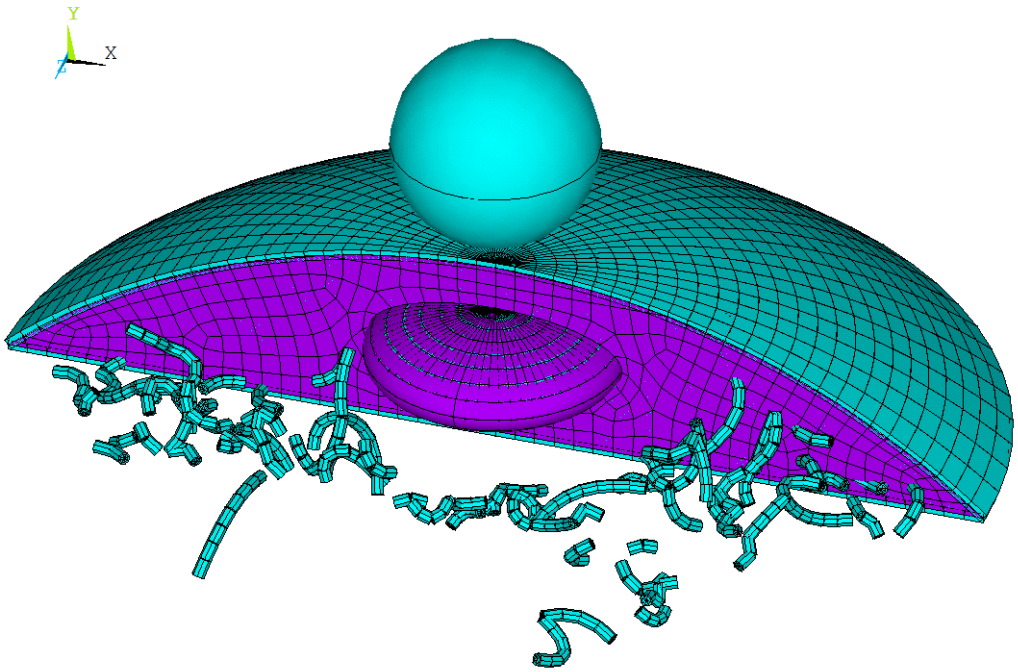

Figure 5.21: The simplifed mitochondrial network incorporated in continuous cell model with AFM indentor at a central position.

of the whole indenter body. Additionally, the contact was considered frictionless with respect to the Hertz theory (and its modified variants commonly used in the experimental environment) utilized in the AFM force-indentation curves conversion.

Another integral part of the problem solution is boundary condition assessment. The mitochondria reportedly attach themselves to the cytoskeleton (either microtubules or actin filaments) [36] in a way that is illustrated in Figure 5.23. Furthermore, they form a bond with the nucleus membrane to perform chemical substance exchange or gene

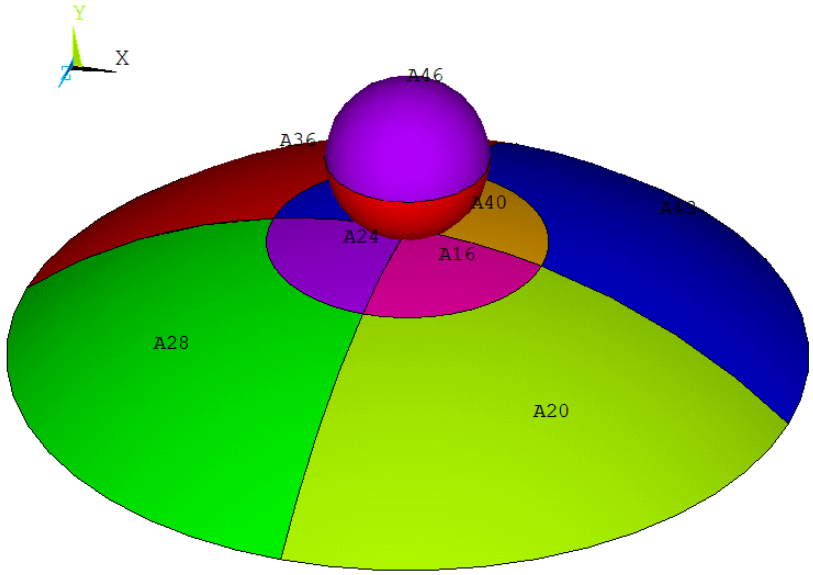

Figure 5.22: Contact problem outline with separated target areas.

transcription [15]. Since the cytoskeleton is not being included in the presented model, the mitochondria were embedded into the cytoplasm using the CP (couple) command. More specifically, the degrees of freedom of each node on the mitochondrion's mid-line (explained above, illustrated in Figure 5.17) are connected with the degrees of freedom of the nearest node in the continuum.

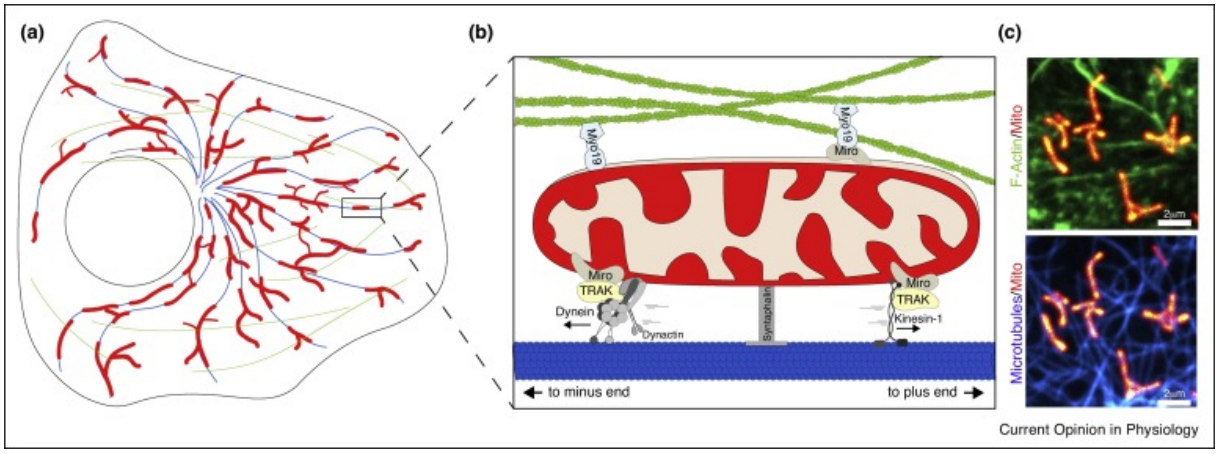

Figure 5.23: Mitochondrial attachments to microtubules (blue) and actin filaments (green). Schematic representation of mitochondrial distribution within cell (a), movement schematics (b) and confocal microscopy images of HeLa cervical cancer cells, source [36].

5.5.1. Evaluation of the cell response

According to the character of the AFM indentation method, the evaluation of reaction force at the indentor tip and of the indentation was performed only at a single direction of an axis determining the cell height (i.e. vertical axis, herein namely as y-axis),

The simulation of the hybrid model proved, that mitochondria do not influence the cell stiffness in a significant way (the difference in the resulting force is equal to 0.3 nN, i.e. 0.05% of the continuum approach only model reaction force) when measured in the central position directly over the highest point as illustrated in Figure 5.22. That is a logical conclusion since most of the mitochondria concentrate around the nucleus however their occurrence is scarce at the "nucleus dominant" site.

The nucleus dominant site is herein used as a designation for the region, where the nucleus determines a significant part of the response of the cell. On the other hand, the response can be defined as "discrete elements dominant" at a sufficient distance from the nucleus meaning that the characteristics or parameters of reinforcing structures such as cytoskeleton or mitochondria are responsible for most of the mechanical behavior. To demonstrate this further, the exterior surface of the previously defined model was loaded by a constant force of 1nN (refer to the Figure 5.24) which can also be interpreted as a gravity-like effect, similar loading conditions also occur while creating force-maps. Notice that the defined areas do not cover all of the cell diameter in the adherent state due to the substantial impact of the substrate at the borderline (periphery).

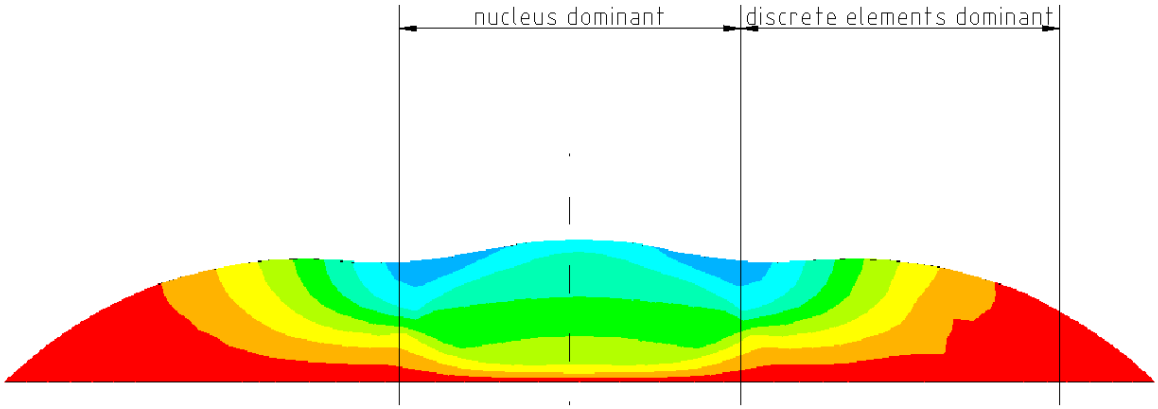

Figure 5.24: Nucleus dominant and cytoplasmatic entities dominant sites designation. Illustrated on a deformed shape of constantly loaded surface as a vertical axis deformation.

This implies, that the assessment of cell mechanical response cannot be evaluated only as a single point measurement. In the experimental approach, the stiffness of the cell is commonly assessed by measuring the response at a series of data extraction points. Those values are subsequently averaged to correspond with overall cell stiffness. A similar approach is applied to the model response measurement as in Figure 5.25.

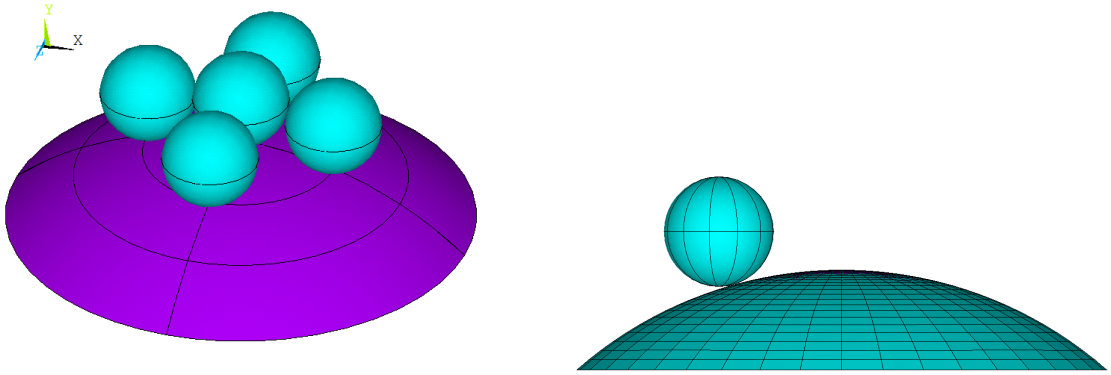

Figure 5.25: Multiple indentation point simulation (left). The response is measured at every indentation point separately so that the individual response curves are not influenced by the other, illustrated on the right.

5.6. Mitochondrial system modification

Manipulation with the mitochondrial network to assess its impact on mechanical response is elaborated on in the following paragraphs. The modifications are generally aimed at evaluating possible pathological effects on the mitochondrial system and all of them were inspired by either changes introduced in literature or other ideas occurring on the basis of natural phenomena, such as bone tissue loss during osteoporosis that can be viewed as constituting network's connection weakening.

To begin with, the most significant objective of studying the mitochondrial attachment in the cytoplasm is, that the number of contact sites reportedly increase during cancer [15]. The impact of such phenomenon can be characterized as mitochondrial fission and fusion imbalance [21], which can be also artificially induced in the cell structure by injection of specific substances such as zinc [38] and thus a state similar to the pathophysiology is induced.

To study this pattern, the number of contact sites in the proposed model was manipulated. This way a number of contact sites and response force were correlated (see Figure 5.26). The number of contact sites is herein being advantageously interpreted as number of divisions (NDIV in the APDL code) along mitochondrial mid-line. The parameter expresses the measure of how mitochondria are bound in the cytoplasm.

The influence of the number of contact sites over the mechanical response of the cell is a non-linear dependency and as such, it can be added to the list of non-linear parameters presented in previous papers (also herein in the Section 5.2.2).

Finally, an additional manipulation with the mitochondrial diameter and its elastic modulus is performed (see Figure 5.26, left) to detect susceptibility to deviations if the parameters are measured (or otherwise determined) in an incorrect way, and the impact of those adjustments on the results. Taking the mitochondrial geometry with two divisions along the mitochondrial mid-line as default (the impact of model modified this way is already substantial in comparison with one contact size, but not overestimated), the initial values are varied to 100%, 150% and 200% to additionally increase the variation. Lower values (e.g. 50%) are not considered, the impact would seem to be negligible and

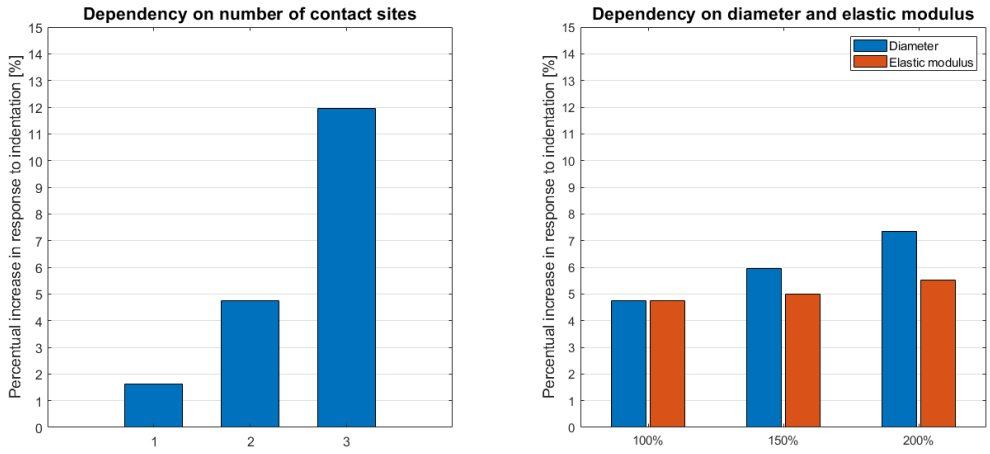

Figure 5.26: Reaction force dependency on selected criteria. Left: number of contact sites (parameter NDIV equal to 1,2 or 3) affecting the cell's response. The reported number of contact sites increase is therefore directly linked to the fact that the overall cell response increases in later stages of tumor progression. Right: sensitivity to other selected parameters.

the information about the significance or non-significance of the variation impact stays the same.

Following the results, the elastic modulus is identified as a non-crucial factor that does not need to be determined with such precision as the number of contact sites or the mitochondrial diameter. However, the latter was measured by a high-precision electron microscope and even though it is represented only by an average value it is considered sufficient for calculations performed herein.

6. Conclusions

The achievements, possible extensions, and/or imperfections of this study are discussed below. To begin with, the objectives evaluation is introduced according to the order defined in the Assignment.

1. *To get acquainted with the structure of an animal cell, especially of its cytoskeleton, with a focus on endothelial cells in blood vessels.*

   A summary of cellular components (their function and arrangement within the cell) was introduced in the initial chapters. Additionally, the list was supplemented with information about cell testing and the mechanical properties estimation for further use was elaborated in an arranged and comprehensible way.

2. *To get acquainted with finite element modeling of pre-stressed tensegrity structures under large deformations.*

   Except for a plain tensegrity and bendotensegrity structures description, a test calculation to demonstrate the impact of pre-stress in cytoskeleton was provided to simulate that the amount of pre-stress introduced to the structure affects the stiffness of tensegrity arrangement.

3. *To simulate a chosen mechanical test of an isolated animal cell using FE model.*

   The proposed model was defined using continuous elements: nucleus, membrane and cytoplasm, wherein the cytoplasm incorporated real-geometry mitochondrial system, the substantial impact of which on whole-cell mechanic response was demonstrated using a simulation of indentation test (AFM).

   The estimated error generated by mesh density [27], the choice of the linear element type or Hertzian contact type can be considered negligible in comparison with other inaccuracies such as in material parameters estimation. The main insufficiency of Neo-Hookean material chosen for the description of the continuous components is considered to be the absence of the strain stiffening, which was detected in comparison with the experimental curve. Mainly the absence of cell cytoskeleton responsible for this phenomenon observed in cell behavior, but also the variability of the reported elastic modulus values thorough the cell spectrum and non-existence of the material model developed for cell behavior description serve to justify this imperfection.

4. *Express inclination towards confirmation or disproval of the hypothesis that mitochondria influence the whole-cell behavior.*

   As demonstrated using the proposed computational model, mitochondria play a fairly significant role in cell mechanical response increasing its stiffness in order of tens percent (approximately up to half the impact of the cytoskeleton), especially when the bonding sites count increases. Since the mitochondria are reported to attach themselves to microtubules and actin filaments to a large extent [36], a FEM model incorporating both mitochondria and cytoskeleton is the next logical step in assessing mitochondrial contribution to cell mechanics.

Several ideas (apart from statistical mechanics implementation to the problem solving which is a wholly new level of assessment, at least for now) for further research and elaboration arose during the development of the novel FEM model introduced herein.

At first, as already mentioned above and since the cytoskeletal components represent around 30 to 40% of the cell stiffness [3] and mitochondria are often bound to cytoskeletal filaments, nucleus, or potentially other cytoplasmic components, a model incorporating both mitochondria and cytoskeleton into cytoplasm volume could be elaborated further. This step would require additional research into the mitochondria-cytoskeleton interaction and possibly a design of additional experimental measurements or inner structure imaging and testing.

The lack of studies dedicated to studying mechanical properties of mitochondria themselves as an individual living cell component gave an incentive to attempt additional experimental measurement aiming at extracting its Young's modulus. As mentioned multiple times, such a task can not be resolved without difficulties such as mitochondria overlap with cytoskeletal components and difficult measurement assembly setup, however matching the mitochondrial mechanical properties with experimental measurements and thus creating a culture-specific FEM model could lead to model's accuracy improvement. Furthermore, mitochondrial variable diameter and curvature along its mid-line was neglected, which could be additionally assessed.

For future reference, mechanical properties in epithelial cells (or their difference from endothelial cells) would need to be researched in more detail and manipulated accordingly. Note that the more cell components are included in the model, the more the cytoplasmic elastic modulus needs to decrease, i.e. the modulus herein referred to as elastic or shear modulus of cytoplasm includes the entirety of the neglected structural components and their possible contribution to the cell mechanics.

The cell shape geometry can be also improved in the future. Approximation of the cell surface (membrane) using a) contact point from AFM microscopy, b) mitochondrial surface geometry or c) confocal microscopy images is possible when aided by programming tools (e.g. herein: a Python code was used for mitochondrial network geometry) as [42].

Two important factors were neglected for the purpose of this research:

- fluid-like (viscous) character of cytoplasm and its compressibility factor

  The impact of the compressibility factor can be easily evaluated by including a material compressibility parameter d into the Neo-Hooke material. The initial estimate of the compressibility factor is equal to roughly a hundred MPa^{-1} (the bulk modulus is larger than the initial shear modulus by approximately two orders).

- and interaction of the proposed model with the surroundings

  That is justified by the scope of the Assignment and the focus on single-cell body interaction with the experimental equipment. Moreover, the examined cells are artificially cultivated and their state during the experimental measurement does not correspond entirely with the physiological state.

Finally, every proposed model needs to appreciate the dynamic and constantly changing nature of the cell's inner structure and the cell as a whole entity. Such parameter is probably not possible to evaluate in any considerable manner (or at least using similar methods as herein).

List of symbols and abbreviations

2D	Two-dimensional
3D	Three-dimensional
AF	Actin fibers
AFs	Actin fibers
AFM	Atomic force microscopy
ATP	Adenosine triphosphate
BUT	Brno University of Technology
DMT	Derjaguin, Muller & Toporov theory
ER	Endoplasmatic reticulum
FE	Finite element
FEM	Finite element method
ID	Inner diameter
IF	Intermediate filament
IFs	Intermediate filaments
MT	Microtubule
MT	Microtubules
MUNI	Masaryk University
NDIV	Number of divisions
OD	Outer diameter
PC-3	Cell culture extracted from human caucasian prostate adenocarcinoma
QPI	Quantitative Phase Imaging
c_{10}, c_{20}, c_{30}	Yeoh material model constants [MPa^{-1}]
d	Compressibility factor [MPa^{-1}]
E	Young's (elastic) modulus [MPa]
F	Force [N]
I_1	First invariant of right Cauchy-Green deformation tensor [–]
$\bar{I}_1$	Modified first invariant of right Cauchy-Green deformation tensor [–]

J	Third deviatoric stress invariant [–]
S	Stiffness [N/m]
W	Strain-energy density function [Pa]
α	Half angle of conical indenter [°]
δ	Indentation depth [m]
ε	Strain [–]
λ	Limiting network stretch [–]
μ, ν	Poisson's ratio [–]
σ	Stress [MPa]

List of Figures

List of Tables

Bibliography

[1] ADAMS, G. G.: The DMT Theory of Adhesion. *Encyclopedia of Tribology*, 2013, Springer US, Boston, MA, p. 3560–3565. DOI: 10.1007/978-0-387-92897-5_499.

[2] ANČÍK, Z.: *Výpočtové modely mechanických zkoušek buněk*. [Bachelor's Thesis] Brno: BUT, FME, 2008. 30 p.

[3] BANSOD, Y. D.: *Computational Simulation of Mechanical Tests of Isolated Animal Cells* [Doctoral Thesis]. Brno: BUT, FME, 2016. 201 p.

[4] BANSOD Y. D. and BURŠA J.: A concise review of soft glassy rheological model of cytoskeleton. *Engineering Mechanics*, 2014, Vol. 21, Issue 4, p. 279–285.

[5] BAUER, D.: *Využití tensegritních struktur pro modelování mechanického chování hladkých svalových buněk*. [Master's Thesis] Brno: BUT, FME, 2011. 73 p.

[6] BURŠA, J., LEBIŠ, R. and HOLATA, J.: Tensegrity finite element models of mechanical tests of individual cells. *Technology and Health Care*, 2012, Vol. 20, p. 135–150, DOI 10.3233/THC-2011-0663.

[7] BURŠA, J.: Learning materials for Biomechanics III., 2020, available at: old.umt.fme.vutbr.cz/ jbursa/

[8] BHAT, N. G. and BALAJI, S.: Whole-Cell Modeling and Simulation: A Brief Survey. *New Generation Computing*, 2020, Vol. 38, p. 259–281. DOI: 10.1007/s00354-019-00066-y.

[9] ČIHÁK, R.: Anatomie 1, Druhé doplněné vydání, Praha: Grada Publishing, 2001. 516 s. ISBN 80-7169-970-5.

[10] CAILLE, N., et al.: Contribution of the nucleus to the mechanical properties of endothelial cells. *Journal of Biomechanics*, March 2002, Vol. 109, Issue 35, p. 177–187. DOI: 10.1016/S0021-9290(01)00201-9.

[11] CLARK, A. G., DIERKES, K. and PALUCH, E. K.: Monitoring actin cortex thickness in live cells. *Biophys J.*, 2013, Vol. 105, Issue 3, p. 570–580. DOI: 10.1016/j.bpj.2013.05.057.

[12] CLARK, M. A., CHOI, J. H. and DOUGLAS, M.: Biology 2e. *Open textbook library*, Edition 2, OpenStax, 2018. ISBN 1947172514, 9781947172517

[13] DENAIS C and LAMMERDING J.: Nuclear mechanics in cancer. *Adv Exp Med Biol.* 2014, Vol. 773, p. 435–470. DOI:10.1007/978-1-4899-8032-8_20

[14] DEGUCHI, S., OHASHI, T., and SATO, M., 2005. Evaluation of tension in actin bundle of endothelial cells based on preexisting strain and tensile properties measurements. *Mol Cell Biomech*, 2(3), p. 125–133. PMID: 16708474.

[15] DESAI, R. et. al: Mitochondria form contact sites with the nucleus to couple prosurvival retrograde response. *Science Advances*, December 2020, Vol. 6, Issue 51. DOI: 10.1126/sciadv.abc9955: EABC9955.

[16] DING, X. et al.: Are elastic moduli of biological cells depth dependent or not? Another explanation using a contact mechanics model with surface tension. *Soft Matter*, 2018, Vol. 14, 7534. DOI: 10.1039/C8SM01216D.

[17] ELDRIDGE, L.: Cancer Cells: How They Start and Characteristics, 2021, available at: verywellhealth.com/what-are-cancer-cells-2248795?print.

[18] ETHIER, C. R. and SIMMONS C. A.: *Introductory Biomechanics*. Cambridge University Press, 2007.

[19] GANGHOFFER, JF., et al.: Prediction of the Effective Mechanical Properties of Regular and Random Fibrous Materials Based on the Mechanics of Generalized Continua. *Mechanics of Fibrous Materials and Applications. CISM International Centre for Mechanical Sciences (Courses and Lectures)*, 2020, Springer, Cham. Vol 596, p. 63-122. DOI: 10.1007/978-3-030-23846-9_2.

[20] GAWAIN, T., et al.: Measuring the Mechanical Properties of Living Cells Using Atomic Force Microscopy. *J. Vis. Exp.*, 2013, Vol. 76, e50497. DOI:10.3791/50497.

[21] GUMULEC, J.: *Interplay between aggressive prostate cancer metabolism and biomechanics – machine learning in quantitative microscopy* [Habilitation Thesis]. Brno: MUNI, Department of Pathological Physiology, 2020. 154 p.

[22] GUZ, N., et al: If Cell Mechanics Can Be Described by Elastic Modulus: Study of Different Models and Probes Used in Indentation Experiments. *Biophysical Journal*, August 2014, Vol. 107, p. 564–575. ISSN: 1751-6161, DOI: 10.1016/j.bpj.2014.06.033.

[23] HARWIG, M., et al: Methods for imaging mammalian mitochondrial morphology: A prospective on MitoGraph. *Analytical Biochemistry*, 2018, Vol. 552, p. 81–99. DOI: 10.1016/j.ab.2018.02.022.

[24] HERMANOWICZ, P., et al.: AtomicJ: An open source software for analysis of force curves. *Review of Scientific Instruments*, June 2014, Vol. 85. DOI: 10.1063/1.4881683.

[25] HOLATA, J.: *Výpočtové modelování mechanických zkoušek hladkých svalových buněk.* [Master's Thesis]. Brno: BUT, FME, 2007. 90 p.

[26] HOLATA, J.: Výpočtové modelování mechanických zkoušek hladkých svalových buněk. *Konference diplomových prací 2007.* Brno: BUT, FME, 2007.

[27] JAKKA, V. and BURŠA, J.: Finite Element Simulations of Mechanical Behaviour of Endothelial Cells. *BioMed Research International*, February 2021, Vol. 2021, Article ID 8847372. DOI: 10.1155/2021/8847372.

[28] JANEL, S., et al.: Stiffness tomography of eukaryotic intracellular compartments by atomic force microscopy. *Nanoscale*, 2019, Vol. 11, Issue 21, p. 10320–10328. DOI: 10.1039/c8nr08955h.

[29] JENSEN, E. C.: Overview of live-cell imaging: requirements and methods used. *Anat Rec*, January 2013, Vol. 296(1), p. 1–8. DOI: 10.1002/ar.22554.

[30] KARCHER, H., et al.: A Three-Dimensional Viscoelastic Model for Cell Deformation with Experimental Verification. *Biophysical Journal*, Nov 2003, Vol. 85, Issue 5, p. 3336–3349. DOI: 10.1016/S0006-3495(03)74753-5.

[31] KRBÁLEK, J.: *Určování elastických parametrů pro modely izolovaných buněk.* [Master's Thesis] Brno: BUT, FME, 2010, 53 p.

[32] LI, Y., et al.: Analysis of mitochondrial mechanical dynamics using a confocal fluorescence microscope with a bent optical fibre. *Journal of Microscopy*, 2015, Vol. 260, Issue 2, p. 140–151. DOI: 10.1111/jmi.12277.

[33] LIM, C. T., ZHOU, E. H. and QUEK, S. T.: Mechanical models for living cells — a review. *Journal of Biomechanics*, 2006, Vol. 39, p. 195–216. DOI: https://doi.org/10.1016/j.jbiomech.2004.12.008.

[34] LEBIŠ, R.: *Výpočtové modelování mechanického chování buňky.* [Doctoral Thesis]. Brno: BUT, FME, 2007. 120 p.

[35] MERZOUKI, A., MALASPINAS, O. and CHPARD, B.: The mechanical properties of a cell-based numerical model of epithelium. *Soft Matter*. 2016, Vol. 12, Issue 21, p. 4745–4754. DOI: 10.1039/C6SM00106H.

[36] MOORE, A. and HOLZBAUR, E. L.: Mitochondrial-cytoskeletal interactions: dynamic associations that facilitate network function and remodeling. *Current Opinion in Physiology*, 2018, Vol. 3, p. 94–100. ISSN 2468-8673, DOI: 10.1016/j.cophys.2018.03.003.

[37] MORIOKA, M., et al.: Microtubule Dynamics Regulate Cyclic Stretch-Induced Cell Alignment in Human Airway Smooth Muscle Cells. *PloS one*, May 2011, Vol. 6. e26384. DOI: 10.1371/journal.pone.0026384.

[38] RAUDENSKÁ, M., et al.: Cisplatin enhances cell stiffness and decreases invasiveness rate in prostate cancer cells by actin accumulation. *Sci Rep*, 2019, Vol. 9, Article n. 1660. DOI: 10.1038/s41598-018-38199-7

[39] SATCHER, R. L. Jr. and DEWEY, C. F. Jr.: Theoretical Estimates of Mechanical Properties of the Endothelial Cell Cytoskeleton. *Biophysical Journal*, July 1996, Vol. 71, p. 109–118. DOI: 10.1016/S0006-3495(96)79206-8.

[40] SCARR, G.: Biotensegrity: What is the big deal? *Journal of Bodywork and Movement Therapies*, 2020, Vol. 23, Issue 1, p. 134–137. ISSN 1360-8592, DOI: 10.1016/j.jbmt.2019.09.006.

[41] SMALL, J. V.: The actin cytoskeleton. *Electron Microscopy Reviews*, Vol. 1, Issue 1, 1988, p. 155–174. ISSN 0892-0354, DOI: https://doi.org/10.1016/S0892-0354(98)90010-7.

[42] SLOMKA, N. and GEFEN, A.: Confocal microscopy-based three-dimensional cell-specific modeling for large deformation analyses in cellular mechanics. *J Biomech*, June 2010, 43(9), p. 1806–16. DOI: 10.1016/j.jbiomech.2010.02.011.

[43] SLOMKA, N., OOMENS, C. W. J. and GEFEN, A.: Evaluating the effective shear modulus of the cytoplasm in cultured myoblasts subjected to compression using an inverse finite element method. *Journal of the Mechanical Behavior of Biomedical Materials*, 2011, Vol. 4, Issue 7, p. 1559–1566. DOI: 10.1016/j.jmbbm.2011.04.006.

[44] STAMENOVIC, D., et al.: A microstructural approach to cytoskeletal mechanics based on tensegrity. *Journal of Theoretical Biology*, 1996, Vol. 181, Issue 2, p. 125–136. DOI: 10.1006/jtbi.1996.0120, ISSN: 0022-5193.

[45] SŮKAL, P.: *Výpočtové modelování mechanických zkoušek izolovaných buněk.* [Master's Thesis] Brno: BUT, FME, 2009, 89 p.

[46] TANG, G. et al.: Biomechanical Heterogeneity of Living Cells: Comparison between Atomic Force Microscopy and Finite Element Simulation. *Langmuir*, 2019, Vol. 35, p. 7578–7587. DOI: 10.1021/acs.langmuir.8b02211.

[47] VARGAS-PINTO, R., et al.: The effect of the endothelial cell cortex on atomic force microscopy measurements. *Biophys J.* 2013, Vol. 105, Issue 2, p. 300–309. DOI:10.1016/j.bpj.2013.05.034.

[48] VEITINGER, T. and JIANG, Z.: Live-cell Imaging Techniques, Visualizing the Molecular Dynamics of Life. Available at: https://www.leica-microsystems.com/science-lab/live-cell-imaging-techniques/.

[49] WANG, N., and STAMENOVIC, D.: Contribution of intermediate filaments to cell stiffness, stiffening, and growth. *Am J Physiol Cell Physiol*, 2000, Vol. 279, p. C188–94. DOI: 10.1152/ajpcell.2000.279.1.C188.